Attachment 8

CDM Apvd

RELEASED
FOR USNRC
REVIEW
2018/01/26

30441R00017
Revision D

REACTOR-BASED MOLYBDENUM-99 SUPPLY SYSTEM PROJECT

ANSYS TARGET CARTRIDGE, HOUSING STRUCTURAL ANALYSIS DESIGN CALCULATION REPORT

Prepared by General Atomics
for the U.S. Department of Energy/National Nuclear Security Administration and Nordion Canada Inc.

Cooperative Agreement DE-NA0002773

[redacted]

GA Project 30441
WBS 1100

GENERAL ATOMICS

MURR® Matters...

nordion

REVISION HISTORY

Revision	Date	Description of Changes
A	24OCT16	Information Issued Initial Release
B	27JAN17	Revised to update the change in cartridge design
C	07FEB17	Incorporated MURR Comments and Updated Table 17
D	26JAN18	Updated references, hot cell layout, cartridge locking and unlocking mechanism, target housing sealing mechanism, and updated FRAPCON analysis with new pellet and cladding tolerances, pellet and cladding roughness, and fill gas composition

POINT OF CONTACT INFORMATION

PREPARED BY:			
Name	**Position**	**Email**	**Phone**
Juan Armando Chavez	Engineer	Juan.Chavez@ga.com	858-455-2465
APPROVED BY:			
Name	**Position**	**Email**	**Phone**
Oscar Gutierrez	Task Lead	Oscar.Gutierrez@ga.com	858-455-3655
Bob Schleicher	Chief Engineer	Bob.Schleicher@ga.com	858-455-4733
Kathy Murray	Project Manager	Katherine.Murray@ga.com	858-455-3272
Katherine Partain	QA Manager	Katherine.Partain@ga.com	858-455-3225

DESIGN CONTROL SYSTEM DESCRIPTION

		DISC	QA LEVEL	SYS
☐	R & D			
☐	DV&S			
☒	DESIGN			
☐	T&E	N	II	N/A
☐	NA			

TABLE OF CONTENTS

LIST OF FIGURES

5a, b, d, e, f

[redacted]

LIST OF TABLES

ACRONYMS

Acronym	Description
ASME	American Society of Mechanical Engineers
FEA	Finite Element Analysis
FEM	Finite Element Model
GA	General Atomics
GPa	Giga-Pascal
kPa	Kilo-Pascal
LEU	Low Enriched Uranium
LWR	Light Water Reactors
MFC	Mass Flow Controller
Mo-99	Molybdenum-99
MPa	Mega-Pascal
MSS	Molybdenum Supply System
MURR	University of Missouri Research Reactor
PSI	Pounds per square inch
RTD	Resistance Thermometer Detector
SGE	Selective Gas Extraction
TA	Target Assembly
TS	Target System

1 INTRODUCTION

The purpose of this document is to present calculation results showing that the Target Assembly (TA) components for the Once-Through Approach as part of the Reactor-Based Molybdenum-99 Supply System (RB-MSS) meet the applicable design requirements of the ASME Boiler and Pressure Vessel (B&PV) Code, Section VIII, Division 1 and 2, 2015 (References 1 and 2) and Section II-B and D, 2015 (Reference 3)

Top level design requirements for the TA are defined in the "Molybdenum-99 Supply System Requirements Document" Doc No 30441S00001.

The Once-Through Approach design will be developed and demonstrated under the RB-MSS project, co-funded by the Department of Energy, National Nuclear Security Administration (DOE-NNSA) and Nordion (Canada), Inc. It is intended that the MSS will be installed and operated at the University of Missouri Research Reactor (MURR) to begin production of commercially-significant quantities of Mo-99 (≥3000 6-day Ci/week) by the beginning of 2018. In addition to a summary-level description of the MSS conceptual design, this document describes the analysis performed to evaluate the performance of the Target Housing, Cartridge, Cladding and Diffuser components that make up the MSS Target Assembly.

2 APPLICABLE DOCUMENTS

A list of applicable documents is provided below.

Document Number	Document Title
30441M00029	Maximum Neutron Damage of Zirc-4, Al 6061-T6 and SS 316
30441R00002	MCNP 6 Version 1.0 Verification Test Report
30441R00020	ANSYS Workbench (Version 16.0) Software Verification Test Report
30441R00021	Target Assembly Thermal Analysis
30441R00028	FLUENT (Version 16.0) Verification Test Report
30441R00031	Mo-99 Target Assembly Nuclear Design for Once-Through Operation
30441R00032	RELAP Accident Analysis and FRAPTRAN Target Rod Transient Analysis Design Calculation Report
30441R00033	Analysis of Forced Convection Cooling of Target Rods with 2 Phase Considerations
30441R00038	Computational Fluid Dynamics Analysis Of Target Housing Design Calculation Report
30441S00001	Molybdenum-99 Supply System Requirements Document
30441S00008	Mo-99 Supply System List of Principal Design Parameters
QAPD-30441-II	Quality Assurance Program Document – Phase II, Reactor-Based Molybdenum 99 Supply System (RB-MSS)

[redacted]

3 DESIGN OF STRUCTURES, SYSTEMS AND COMPONENTS

3.1 SGE Experimental Facility Description

The SGE experimental facility employs a first-of-a-kind concept for radioisotope production. It is a reactor-driven, LEU based system that selectively removes specific isotopes of interest, viz., Mo-99, in gaseous form, that are produced from fission during irradiation of Zircaloy-4 clad target rods containing LEU in the form of UO_2 pellets that are nominally enriched to 19.75% U-235. The target rods will be contained in Al6061 cartridges that ensure uniform cooling water flow around the target rods and will be located in the graphite reflector region of the 10 MW University of Missouri Research Reactor (MURR). The SGE facility will be operated by MURR staff in concert with MURR's routine reactor operations.

During SGE system operation, one or two target cartridges holding up to 11 target rods each are placed in permanently installed support assemblies in the graphite reflector location. Fission product isotopes including Mo-99 are generated during target irradiation. At the end of irradiation ([redacted]), the target rods, following a short period of cooling (to reduce decay heat and certain short lived isotopes), are removed and transferred to a bank of hot cells using an intra-facility, shielded transfer cask, also designed for adequate heat dissipation during transfer. Here, the irradiated target rods are decladded to remove the irradiated UO_2 pellets, which are then subject to the selective gaseous extraction process (SGE) to separate the Mo-99 in gaseous form to a collection apparatus. The product is then further processed to separate molybdenum from the collection process by-products and impurities. The product is then packaged and shipped to a licensed radioisotope facility for final purification that meets the required U.S. Food & Drug Administration (FDA) purity standards for fabrication of Tc-99 generators. The residual uranium-containing powder is reduced to UO_2, encapsulated and placed in sealed storage containers for eventual disposal.

5a, d, e, f

The fully-loaded target cartridges themselves are each, and together, subcritical in water ($k_{eff} < 0.8$) as detailed in 30441R00031. Fission only occurs in the target when exposed to neutron irradiation from the reactor.

Figure 1 shows a functional block diagram of the SGE process including process streams, subsystem and interfaces with the reactor and containment facility.

[redacted]

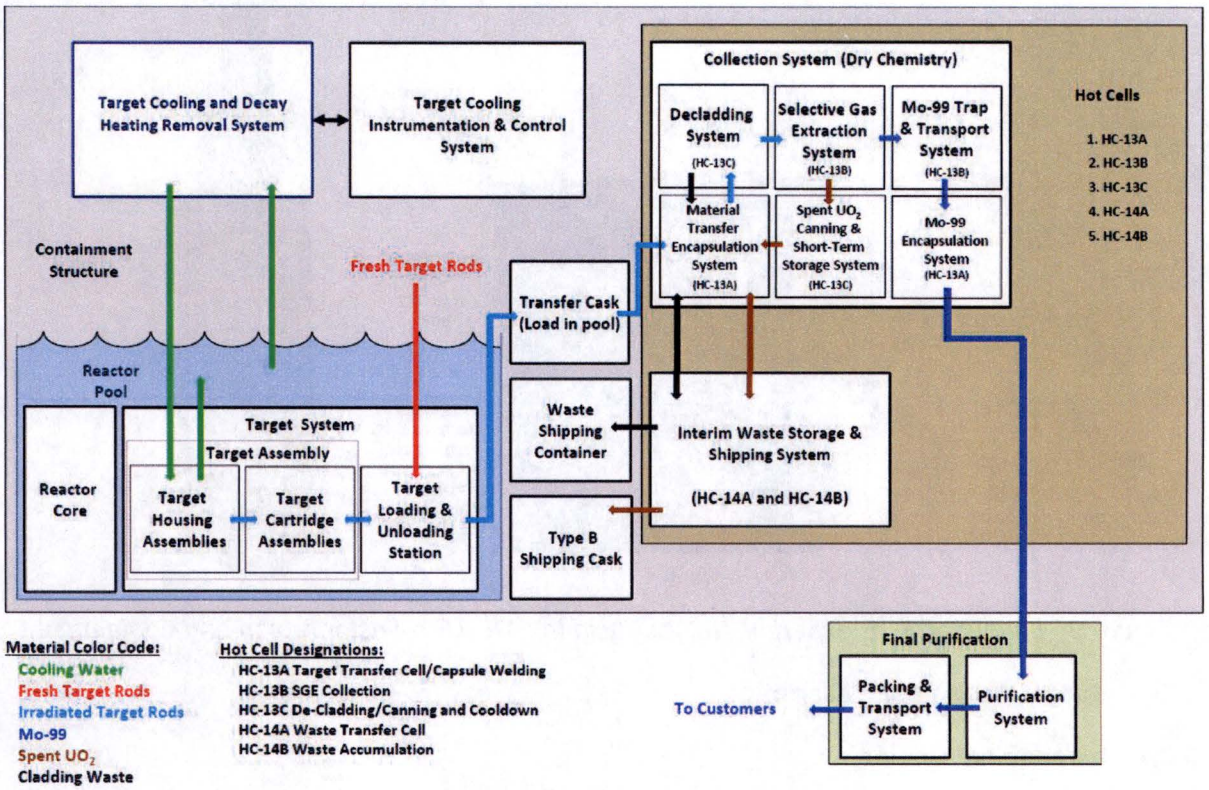

Figure 1. SGE process scope, functional relationships and interfaces

The SGE facility is divided into separate subsystems. The Target System includes a Target Assembly and a Target Loading and Unloading station. The Target Housing is described in Section 3.2.2. The Cartridge Assembly is described in Section 3.2.3. Figure 2 shows a layout of the SGE systems within the MURR reactor pool and containment building. The cartridge loading station is where the target rods are removed from the cartridge and placed in a transfer cask. The cartridge is reloaded with fresh or dummy target rods in this location.

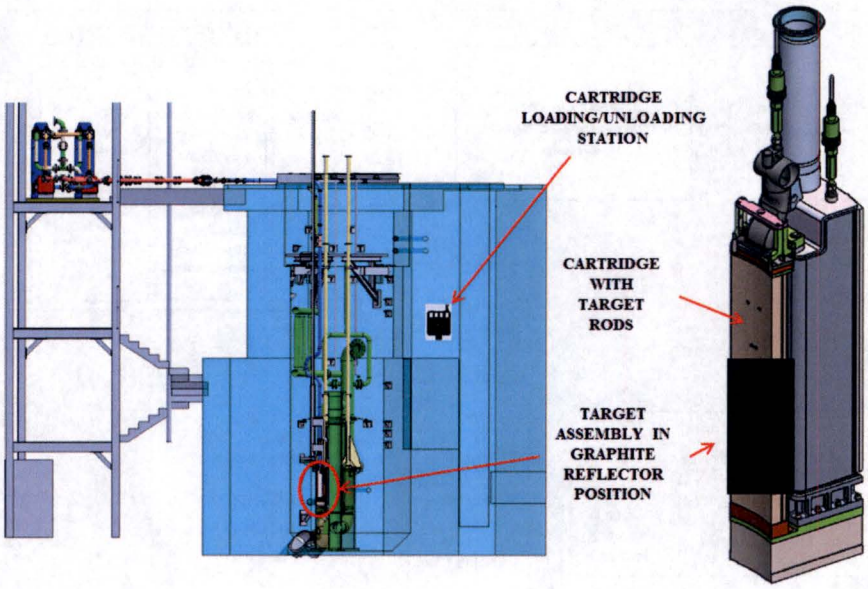

5a, b, d, e, f

Figure 2. Layout of SGE experimental facility in the MURR reflector region and containment

3.2 Target Assembly Description

3.2.1 Mechanical Design

The target assembly (TA) is designed to be installed in each of the reactor graphite reflector positions 5A and 5B as shown in Figure 3. The housing is held laterally in place by an indicator hole in the reactor baseplate and vertically in place by the target cooling system inlet pipe which includes a compressible link. Each target assembly consists of a water inlet section, a target housing, a lower plenum, a cartridge assembly, an outlet diffuser, and a cartridge locking mechanism. Figure 4 shows the target assembly components. The modeling and mechanical design of the target assembly components in 3D was performed using the commercially available SolidWorks 2016 software package.

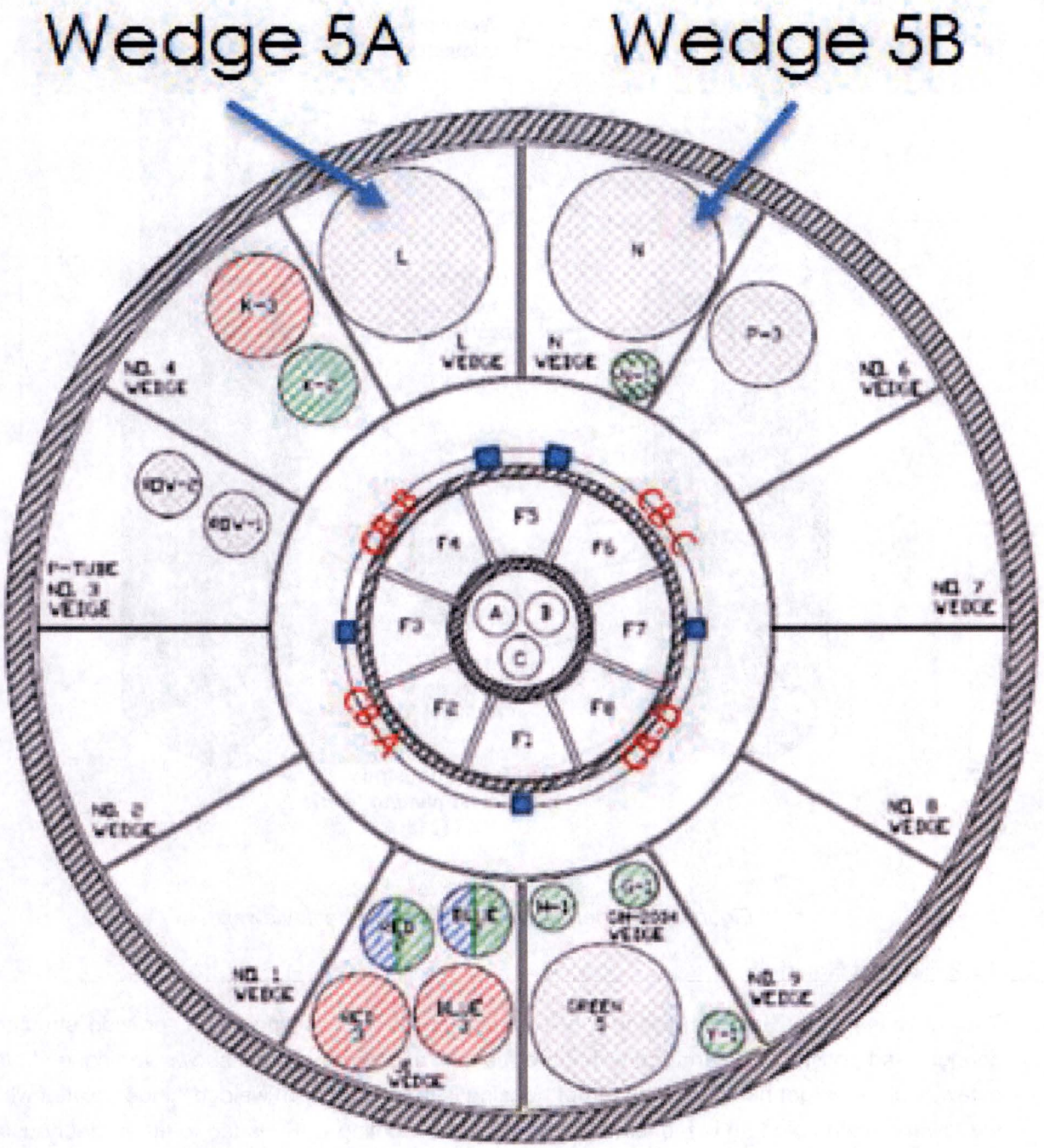

Figure 3. MURR map for fuel elements and reflector regions

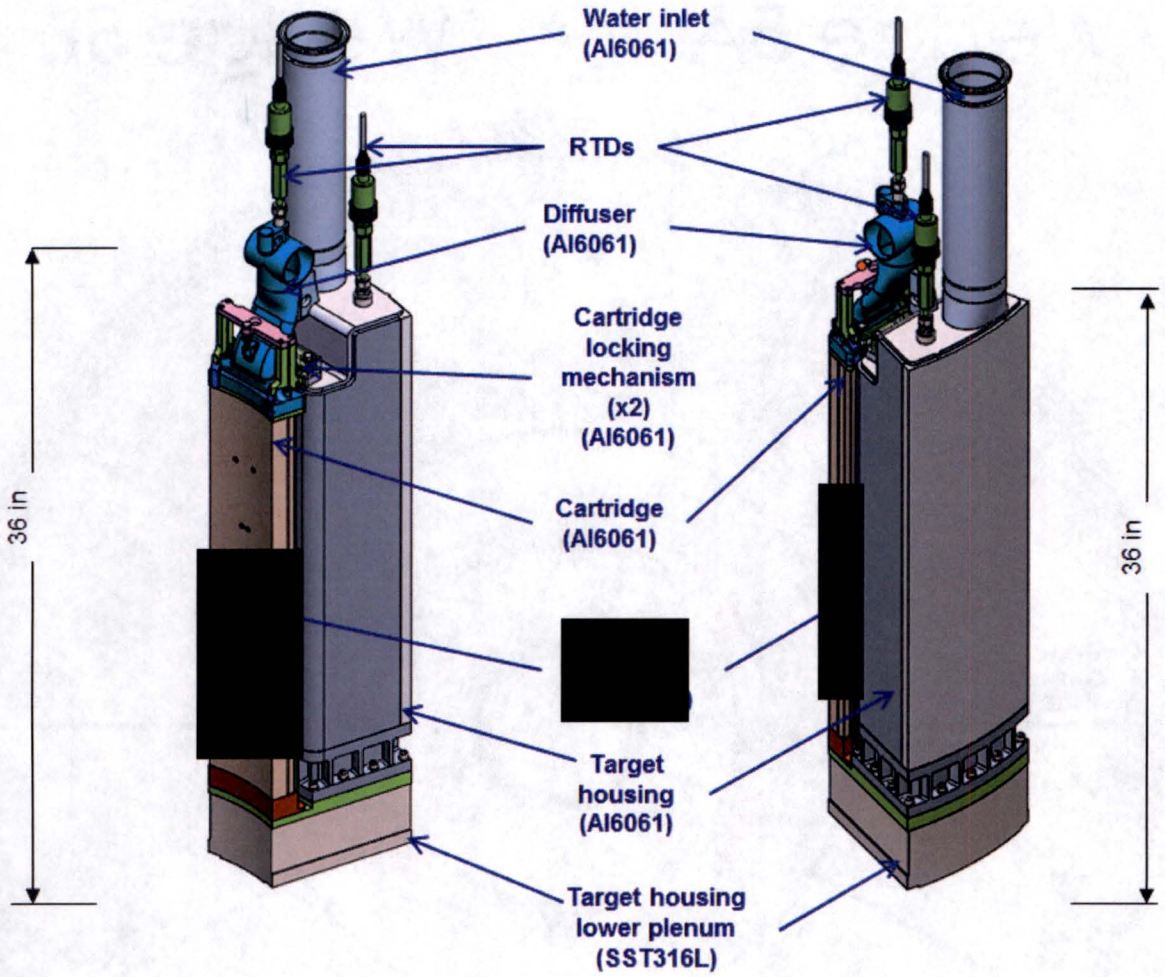

5a, b, d, e, f

Figure 4. Target assembly (front and back views)

3.2.2 Target Housing

The functions of the target housing are to direct the flow of cooling water, provide structural support, and position the cartridge within the reactor reflector. Figure 5 shows vertical and plan cutaway of the target housing. The target housing is fabricated from welded Al6061 plates while the lower housing plenum is fabricated from SS316L. Cooling water is fed to the target housing by the target cooling system through a line at the top of the assembly. The target housing then directs the water down through the lower plenum, up the inside of the cartridge and finally exiting out the diffuser into the MURR pool. The target housing and the lower housing plenum are bolted together and water leakage is prevented by a metal e-seal that keeps this interface water tight.

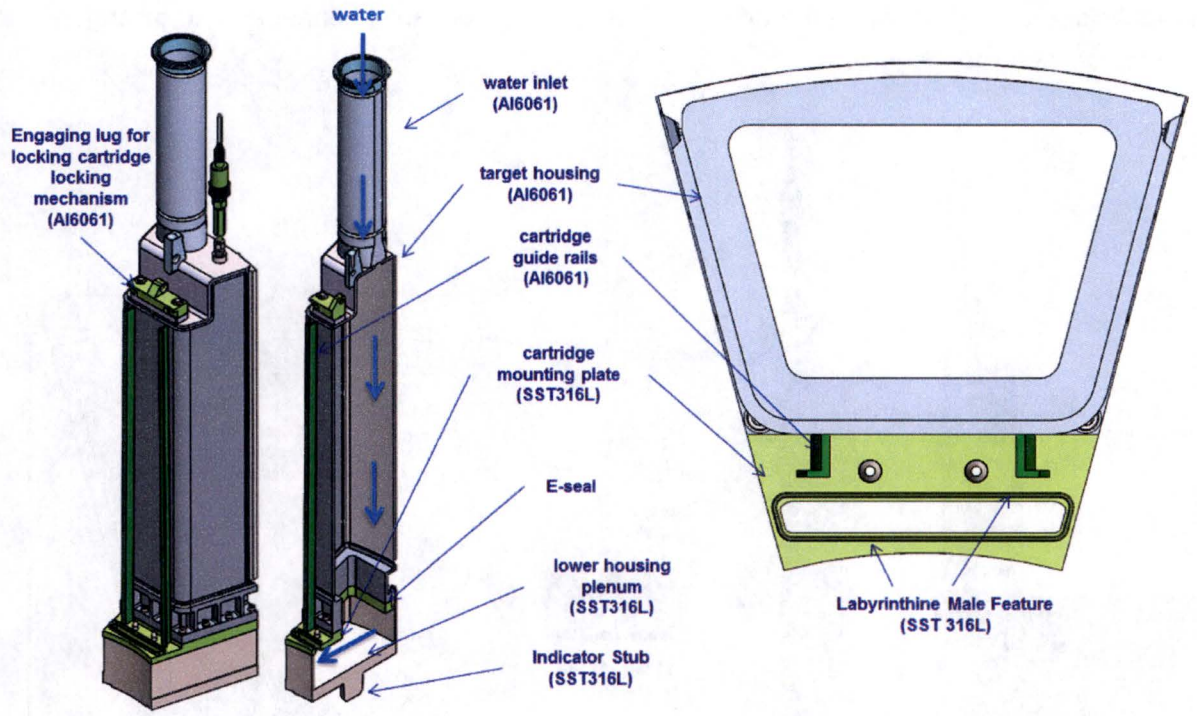

Figure 5. Illustration of target housing assembly elevation and plan views

The bottom of the housing has a locator stub that fits in the reactor support structure, which bears the weight of the assembly and attached piping. The load from the piping is transferred to the lower housing plenum by the target and the housing sides. The lower housing water plenum is bolted to the target housing with an e-seal to prevent loss of cooling water before reaching the cartridge and the target rods.

3.2.3 Target Cartridge Assembly

3.2.3.1 Cartridge

The primary functions of the cartridge are to (a) position and support the target rods containing the LEU pellets, (b) provide a cooling passage for the target rods, (c) [redacted] and (d) to mix and guide the water outlet flow. The cartridge assembly consists of an Al6061 diffuser on the top, an Al6061 cartridge flow housing, [redacted] an Al6061 lower cartridge flange, a locking mechanism, and 11 single Zircaloy-4 clad target rods. The target rods are vertically oriented in a single plane positioned in the target cartridge orthogonal to the direction of the neutron flux (Figure 6). The planar orientation and location ensures the SGE facility maximizes the Moly-99 production while remaining sub-critical. The target rods are held in position by the top and bottom cartridge flanges which contain holes for the coolant to flow around the target rods. The cartridge is secured in place by a locking

5a, b, d, e, f

mechanism located on top of the diffuser. The locking mechanism engages and disengages to the top of the target housing.

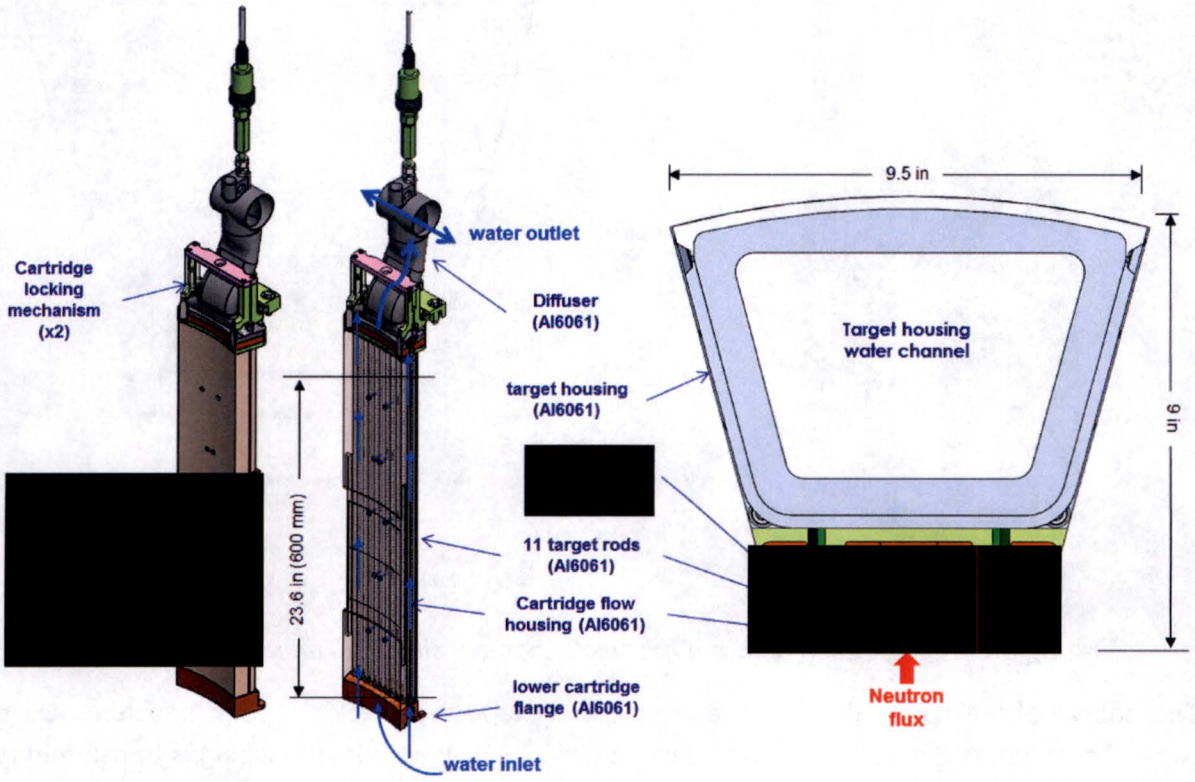

5a, b, d, e, f

Figure 6. Target cartridge assembly and target assembly section view

Figure 7 shows the cartridge upper and lower sections highlighting key components and features of the design. The cartridge is a clamshell design that will have two seam welds running the length of the cartridge. This simplifies the fabrication as well as allowing more control over the tolerances for the fit between the water cooling channels and the target rods. The cartridge is first located to the target housing by a pair of guide rails that lead to a unique labyrinthine male feature (Figure 5). This feature is part of the target housing lower plenum and receives and places the cartridge in its final position in relation to the reactor core. The cartridge is then held in place by a locking and unlocking mechanism that releases the cartridge from the target housing, consisting of couple of levers actuated by two spring loaded bolts that hold the pressure and water flow loads of the target assembly and is explained in more detail in Section 3.2.4.4.

5a, d, e, f

Figure 7. Target assembly upper and lower sections

The target rods are fixed on the top (upper endcap) and laterally restrained at the bottom (lower endcap) allowing room for axial thermal expansion . The target rods are expected to thermally grow by < 2 mm, leaving for margin including mechanical tolerance stack-ups. The target rods are located and held concentric to the water channels by 11 cup features that are fabricated into the lower cartridge flange and can be seen on Figure 8. Target rod lower end cap pins position rods relative to the lower housing water plenum. This ensures even flow velocities around the target rods through the cartridge. The water cutouts on the cup features are smaller than the pointed end cap of the target rod. This eliminates the possibility of the target rod getting stuck on one of these water bypass features when inserting them into the cartridge and ensures the worker can always find the center of the cartridge and guide the target rod into its final position.

5a, b, f

5a, b, d, e, f

Figure 8. Target rod lower end cap pins position rods relative to lower housing water plenum

The water cutouts are designed to create near-uniform coolant flow over the target rods as soon as the water enters the cartridge.

5a, b, d, e, f

5a, b, d, e, f

3.2.3.2 Target rods

The function of the target rod is to contain the UO_2 target pellets and to prevent fission gas release. Figure 10 shows an individual target rod assembly. The target rod consists of an upper end cap, cladding, a spring, one hundred [redacted] UO_2 target pellets, and a lower end cap. [redacted] The UO_2 target pellets have a nominal active length of 23.6 inches (600 mm) in the cold state. A nominal radial gap of 50µm exists between the pellet OD and the cladding ID. This nominal gap offers the best dimensional balance between cladding strain and thermal conductivity to the cladding wall. The end caps are fabricated from Zircaloy-4 bar with integrated features designed to optimize installation and extraction from the cartridge. Both end caps are welded to the cladding autogenously (no filler rod) by a standard automated orbital weld head. The stainless steel spring is held captive by the upper end cap, to aid in easier recovery post-irradiation. Table 1 lists the individual pellet/clad components and dimensions.

5a, d, e, f

The Zircaloy-4 (UNS R60804) cladding will be fabricated and inspected in accordance with seamless alloy tubes for nuclear reactor fuel cladding applications per American Society for Testing and Materials (ASTM) B811. The Zircaloy-4 (UNS R60804) end caps and stainless steel spring will be fabricated from bar material in accordance to ASTM B351.

[redacted]

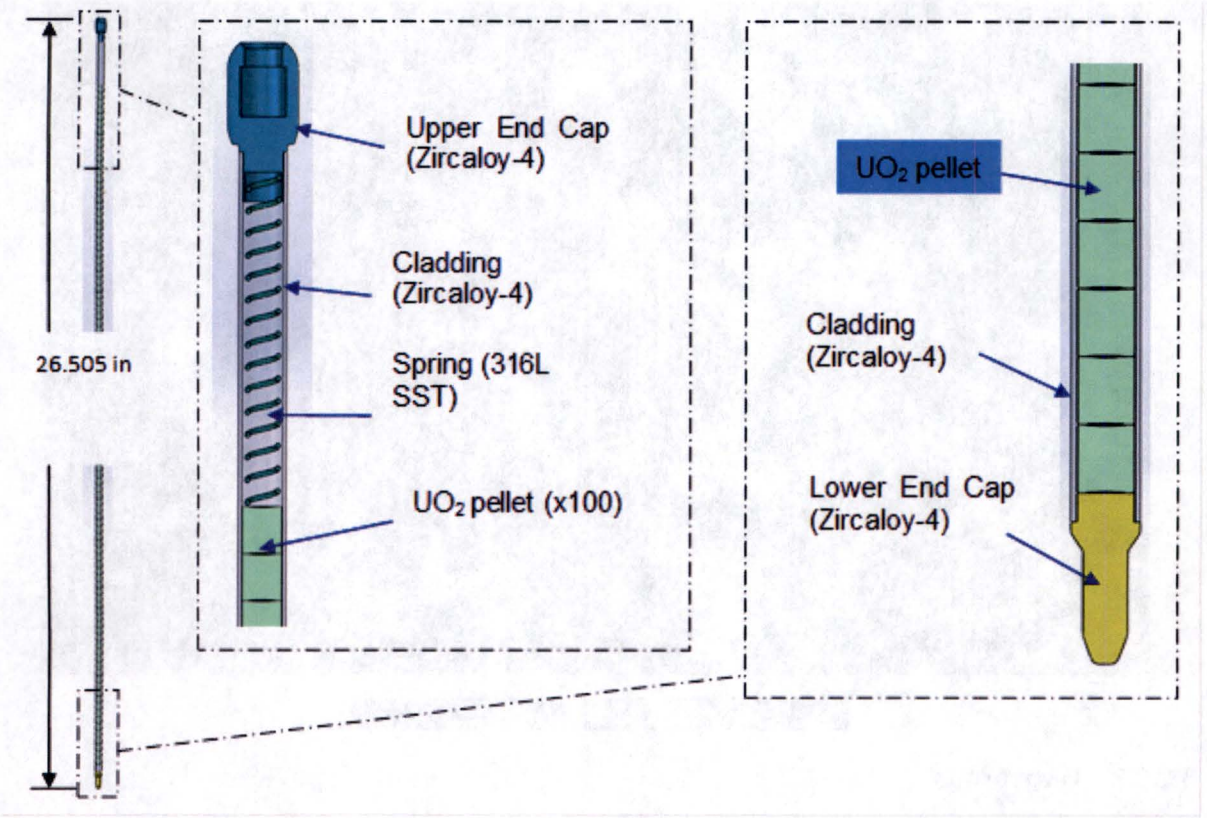

Figure 10. Target rod arrangement

Table 1: Target Rod Dimensions (Cold)

Component	Nominal value inches (mm)
Active target rod length (cold)	23.6 (600)
Total target rod length	26.505 (673)
Pellet height	0.236 (6)
Pellet outside diameter	0.197 (5)
Clad ID	0.201 (5.1)
Clad OD	0.240 (6.1)

3.2.3.3 Diffuser

The functions for the diffuser are a) to capture the target rods (Figure 7), b) provide water mixing for an outlet water temperature measurement, c) divert the flow away from MURR equipment, and d) to guide ^{16}N flow away from the pool surface. The water is mixed in the diffuser's water flow mixing region (Figure 11) to allow for a bulk water temperature measurement. The exit temperature measurement is used to determine the Target System power.

3.2.4 Cooling Flow Path

3.2.4.1 Target Water Flow Path

Figure 11 shows the path of cooling water flow in the target system. Cooling water enters the housing from the inlet pipe and flows into the open lower plenum turning into the lower cartridge flange. The lower cartridge flange has labyrinthine features to minimize water bypassing the target rods during normal operations. The flow then travels around the target rods, into the diffuser and is ultimately ejected to the reactor pool.

5a, b, d, e, f

Figure 11. Inlet and outlet plenum extensions with method of attachment. Water flow is in blue

3.2.4.2 Lower Target Housing and Cartridge

Figure 12 shows a cross-section of the target housing lower water plenum. The bottom of the housing has a locator stub that fits in the reactor support floor, which bears the weight of the

assembly and attached piping. The load is transferred to the target bottom through the housing sides. The target rods are supported from upper cartridge flange and simply supported from the bottom endcaps by the lower cartridge flange, which also provide the target rods with concentricity to the cartridge water channel (with margin for thermal growth). The lower housing water plenum is bolted to the target housing. This interface is then sealed with a c-seal to prevent loss of cooling water before reaching the cartridge and the target rods.

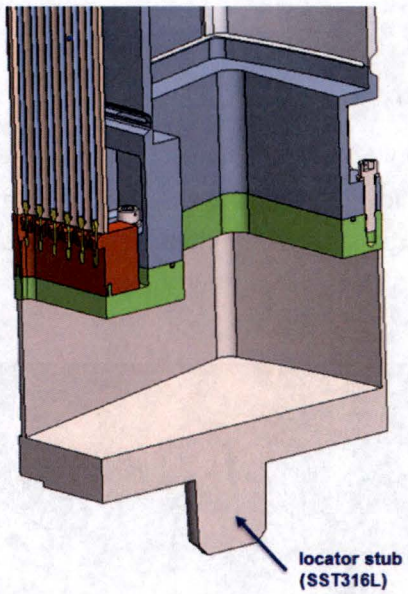

Figure 12. Lower target head

3.2.4.3 Upper Target Housing and Cartridge

Figure 13 shows the upper target housing, cartridge, and lower section of the diffuser. The lower flange of the diffuser acts as the lid that holds down the target rods and keeps them from coming out of the cartridge by capturing the target rod's upper end cap. This, along with the lower cartridge flange supporting the target rods, properly constrains the target rods through the installation, irradiation, and transfer to the temporary holding area inside the pool. The lower diffuser flange is welded to the neck portion of the diffuser, which collects the water exiting the cartridge and mixes it together before guiding it to the resistance temperature detector (RTD) for measurement and ultimately to the pool. The mixing of the flow is very important to be able to take an accurate measurement of the power being generated by the target assembly, particularly when not all of the target rod positions are filled with LEU rods. Mo-99 production may require anywhere between 3 to 11 target rods to be irradiated at a time, with the rest being dummy rods. The water flowing over the dummy rods will exit into the diffuser much cooler than the water from the actual target rods, thus mixing of the flow is critical for an accurate power

measurement. At each interface, cartridge flange to lower diffuser flange to diffuser ducting, the water cross-sectional area remains constant.

5a, b, d, e, f

Figure 13. Upper target head arrangement. Water flow is in blue

This allows the diffuser to have a minimal pressure drop from the cartridge exit to the reactor pool.

When it is time to remove the irradiated cartridge from its irradiation position in the reflector for transfer to the in-pool loading/unloading station, the cartridge will be maneuvered and handled remotely in the reactor pool by the operator positioned on top of the pool. The cartridge is moved from the reflector wedge to the in-pool unloading station, where the diffuser is unlatched from the cartridge to access the target rods for loading into the transfer cask. The diffuser is attached to the cartridge by using two positive lock, spring loaded, quarter turn, cam lock bolts that engage to the cartridge upper flange. The two bolts are readily accessible and visible from the top by the operator and tools have been developed to perform such a function within the reactor pool.

3.2.4.4 Cartridge Locking Mechanism

The locking and unlocking mechanism that releases the cartridge from the target housing consists of couple of levers actuated by two spring loaded bolts that hold the pressure and water flow loads of the target assembly. As seen in Figure 14, the holding levers are controlled by the two bolts that slide laterally when the bolts are rotated which in turn makes the lever pivot to clear the locking lug attached to the target housing. This releases the cartridge to be lifted to the unloading/loading zone higher up in the pool. These two 1/4-20 bolts are more than enough to restrain the cartridge from the anticipated vertical load from the flow of 15-20N and thus making this a secured experiment.

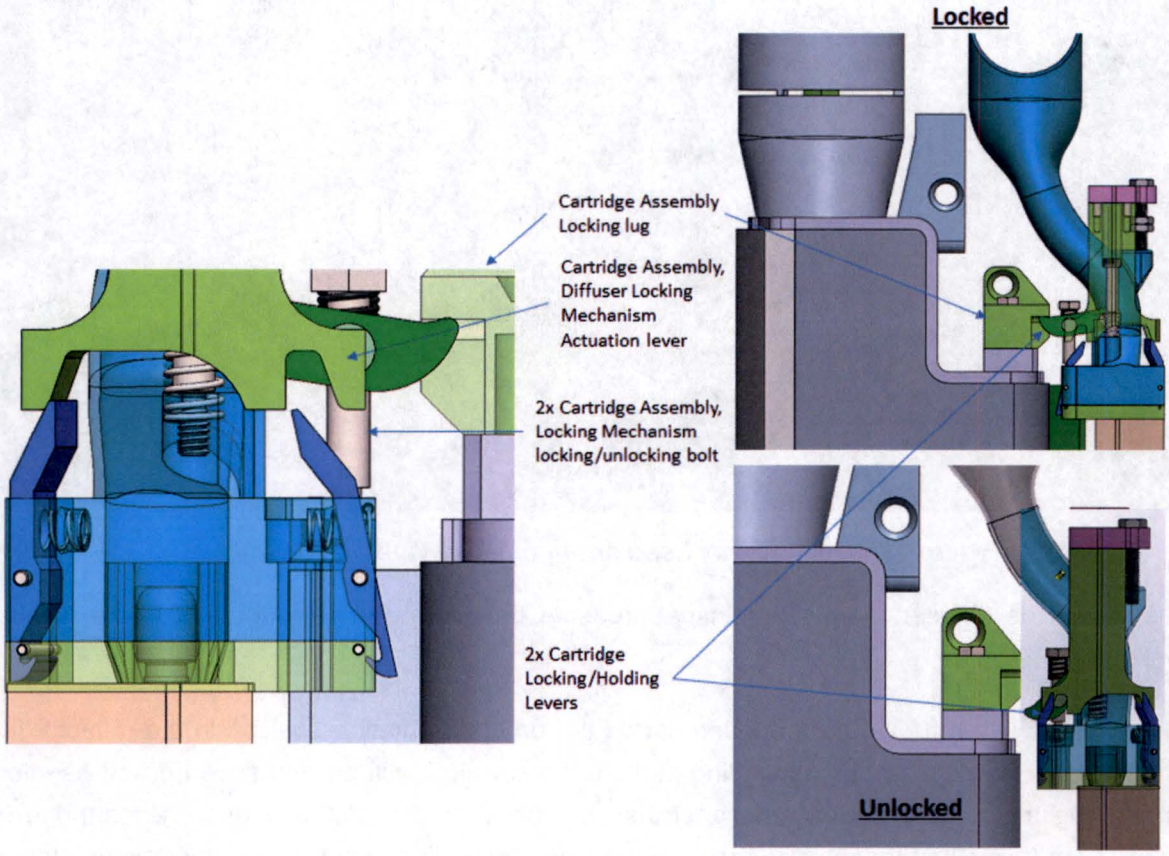

Figure 14. Locking and unlocking mechanism

3.2.5 Materials of Construction

3.2.5.1 Design Basis for Target Assembly Materials

The considerations upon which target assembly material selections are based are as follows:

(i) Prior operating experience for target cladding materials in a nuclear reactor irradiation environment is preferable.

(ii) The materials must have good mechanical strength at temperature up to 400°C.

(iii) Materials in the neutron flux must have low neutron absorption cross-sections so as not to impede the rate of Mo-99 production.

(iv) Selected alloys must have the properties to support readily fabrication into required shapes and must be readily weldable.

(v) The material used for the inner clad of the target rod must not undergo undesirable chemical reactions with the target pellet material or fission products within the operating temperature range.

3.2.5.2 NRC-Approved Fuel Cladding Alloys

Alloys that have been approved by the Nuclear Regulatory Commission (NRC) for fuel cladding in power and research reactors in the United States include Zircaloy, SS304, SS316L, and Al6061. Zircaloy-4 is the preferred candidate due to its lower neutron absorption, which results in higher product yield, and is also used in LWRs. The Zircaloy-4 (UNS R60804) cladding will be fabricated and inspected in accordance to seamless alloy tubes for nuclear reactor fuel cladding applications per ASTM B811.

4 CODES AND STANDARDS

4.1 Design, Fabrication and Operation

General Atomics (GA) is the prime contractor for the design and supply of the SGE experimental facility structures, systems and components (SSC). The SGE experimental facility will be designed and fabricated in accordance with applicable codes and standards, specifically:

- The SGE experimental facility structures, systems and components (SSC), and conduct of operations with the facility, shall comply with all applicable USNRC reactor license requirements, other federal regulatory requirements, as well as local and state design codes and standards requirements.
- SGE experimental facility components shall be designed to meet the applicable requirements in Section VIII, Div. 1 & 2 of the ASME B&PV Code, 2015 (References 1 and 2).
- Welding shall meet the applicable requirements[1] in Section IX of the ASME B&PV Code, 2015 (Reference 4).
- Weld NDE shall meet the intent of the applicable requirements in Section V of the ASME B&PV Code, 2015 (Reference 5).

[1] The applicable SSCs of the SGE experimental facility will be designed to meet all the requirements of the ASME code, but will not be code certified SSCs.

- All materials used in SGE experimental facility components shall meet the intent of applicable requirements in Section II of the ASME B&PV Code, 2015 (Reference 3).
- Regulatory Guide 2.2, Development of Technical Specifications for Experiments in Research Reactors, U.S. Atomic Energy Commission, November 1973, (Reference 6).

4.2 Software

The nuclear, thermal hydraulic and mechanical design of the SGE experimental facility utilized the following analytical and design software packages.

- RELAP5 to confirm thermal hydraulic parameters of the target assembly, and for analysis of target transient conditions.
- FRAPTRAN for source term calculation verification (transient analysis)
    - RELAP and FRAPTRAN Accident analysis is reported in GA Doc. No. 30441R00032 "RELAP Accident Analysis and FRAPTRAN Target Rod Transient Analysis"
- FRAPCON for source term calculation verification (steady state analysis)
- ANSYS Workbench R16 was utilized for the structural performance analysis for the target assembly
    - ANSYS Workbench R16 software was tested and verified with GA Doc. No. 30441R00020 documenting the results of the software with GA computers.
    - For the fluid analysis portion of the analysis, ANSYS FLUENT was tested and verified with GA report 30441R00028 documenting the results.
- SolidWorks 2016 for the detailed mechanical design and 3D visualization.

The use of all software for the development of the SGE experimental facility has been subjected to the rigorous software quality assurance (QA) verification and validation procedures as required by the GA Quality Assurance Program and related documents (QAPD-30441-II), including preparation of verification and validation reports as required by the applicable requirements in the applicable engineering procedures in Reference 1.

5 DESIGN INPUTS

The Target Assembly (TA) geometry design and dimensions are based on "Molybdenum-99 Supply System Requirements Document", Doc. No. 30441S00001 and is described in Section 5.1. Design conditions for specific assembly components are summarized in Section 5.1. Materials of Construction for the main assembly components are listed in Table 3 in Section 6. There was no corrosion allowance for the design (preliminary test samples placed

inside the MURR Pool only showed appropriate levels of oxidation). Images documented are on APPENDIX A.

5.1 Mechanical Design

The target assembly (TA) is designed to be installed in one or more of the reactors graphite reflector positions. A maximum of two TSs - #5A and #5B - will be installed as part of the SGE facility. Each TA consists of a water inlet section, a target housing, a lower plenum, a cartridge assembly, an outlet diffuser, and a cartridge locking mechanism. Figure 4 shows the TA components. The modeling and mechanical design of the TA components in 3D was performed using the commercially available SolidWorks 2016 software package while the analysis of the components was performed with ANSYS Workbench R16 (30441R00020) of which results are presented in Section 7. The Target Assembly design pressure inputs will vary across the sub-components due to the pressure drop that the cooling water will see as it moves through the system. To quantify the actual pressures each component will see during normal operating conditions, an ANSYS Fluent Analysis model was developed to calculate this pressure drop. All of these calculations and parameters are detailed in Doc. No. 30441R00038. Figure 15 was made by extracting the pressure drop parameters from 30441R00038 for reference for the 100% & 115% flow cases. Section 7 has the detailed stress analysis for all components in the Target Assembly.

The water flow enters the target housing through a 3" pipe that is called position one in Figure 15 below (position 1). The flow makes its way through the housing and around the lower plenum and makes its way up, through the lower part of the cartridge flange (position 2). The flow then moves around the grid features that keep the target rods concentric to the cartridge water channels and reach the cartridge main target cooling zone (position 3). The flow makes its way around the targets, cooling them until it reaches the top of the cartridge (position 4) and makes its way through the cartridge top flange grid that holds the target rods in place. Once outside the cartridge (position 5), the diffuser assembly takes over and guides the water flow to the eventual exit location and into the pool (position 6). For this analysis, the pool pressure at the exit of the diffuser is 0 psi meaning that the pressure loads are the difference between the total pressure and the Outlet Static Pressure of the Target Assembly. The pressures for the target assembly loading are summarized in Figure 15.

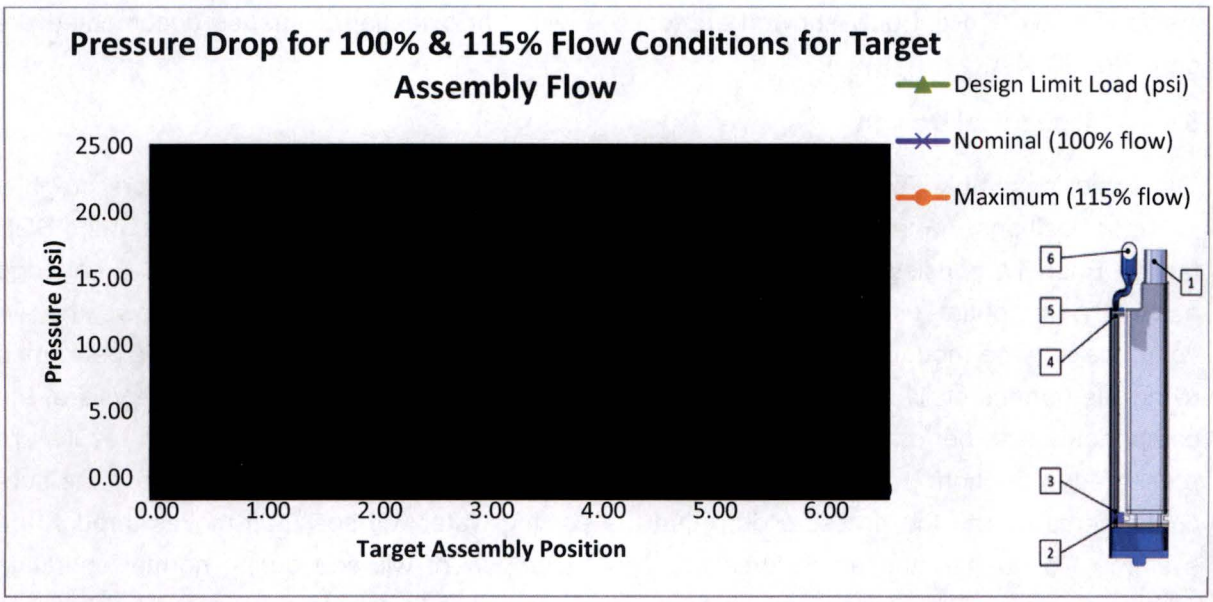

5a, d, e, f

Figure 15. Total pressure minus outlet static pressure cooling water through target assembly from point 1 to 6 at 100%, 115% flow vs max design conditions. Taken from 30441R00038.

These numbers are the maximum loading design parameters for the housing and the cartridge. 21.5 psi [148.23 kPa] for the Housing and 14.8 psi [102.04 kPa] for the cartridge are maximum loading conditions (at locations shown) that meet the ASME B&PV Code allowables as defined by Figure 16 in Section 7.1 as well as maintaining a minimum factor of safety of 2 per NUREG 2.2 (Reference 6). Although it is not expected to see values above the 115% flow case, these design values are 25.8% (for the Housing) and 21.7% (for the cartridge) higher than the 115% flow case, more than satisfying the requirements. The detailed stress analysis results for all the TA components are presented in Section 7.

Table 2: Target Assembly Loading

	Loading (psi)		Loading (kPa)
Max Design Pressures for TA components	Housing	21.5	148.23
	Cartridge	14.8	102.04

5.1.1 Target Housing

Figure 15 shows that the ANSYS FLUENT analysis (30441R00038) yielded a pressure of 17.42 psi [120.11 kPa] for the highest flow case of 115%. The Target Housing however will be analyzed for the loading condition from Table 2 and a factor of safety will be obtained by

comparing the Target Housing stresses to the ASME Ultimate Tensile Strength allowable at temperature to see that it satisfies NUREG 2.2 (Reference 6) as defined in Section 7.1 below.

5.1.2 Cartridge Assembly

Figure 15 shows that the ANSYS FLUENT analysis (30441R00038) yielded static a pressure of 12.16 psi [83.84 kPa] for the highest flow case of 115%. The actual pressure drop though the target rods and the cartridge is 3.28 psi [22.61 kPa] (between positions 3 and 4), the rest of the pressure drop comes from the target rod support flange on the outlet of the cartridge and diffuser (positions 5 - 6). The Cartridge Assembly will be analyzed for the loading condition from Table 2 and a factor of safety will be obtained by comparing the Cartridge stresses to the ASME Ultimate Tensile Strength allowable at temperature to see that it satisfies NUREG 2.2 (Reference 6) as defined in Section 7.1 below.

5.1.2.1 Target Rods

Per design requirements (30441S00001), target rods can be irradiated over a 3 week period before they are pulled for further processing, with mid-week and end of week shutdowns over that period. The reactor nominal operating power is 10MW (100%). Though unlikely, the reactor can conceivably drift up to 11.5MW (115%) reactor power before the control system will take action and lower the control blades.

To look at pellet-cladding interaction, hence pellet thermal and cladding structural performance, the target rods were analyzed using FRAPCON. The analysis was performed for three different UO_2 to Cladding gap sizes, [redacted] (Min.), 50 µm (Nom.) and [redacted] (Max.), for a 3 week operational period, with the reactor power being set at 100%, except of the first and last day, where the reactor power is assumed to be at 115% for conservatism. This sequence provides the most conservative results for temperatures, fission gas release and relocation. For further details refer to Section 7.2.2.2. 5a, d, e, f

To look at vibration of the target rods, and according to the report ANL-GenIV-070 - Generation IV Nuclear Energy System Initiative Pin Core Subassembly Design, p. 57 (Reference 7), there are two primary concerns from the viewpoint of vibration analysis: i) the magnitude of turbulence-induced target rod displacements (i.e., preclude rod-to-rod contacts which could result in damage accumulation over the course of plant operations); and ii) excitation mechanisms, wherein the frequency of flow field oscillations may match the natural vibration frequency of the target rods, resulting in energy extraction from the flow field that can lead to rod damage. These two points are addressed in Section 7.2.2.2.3.

Bowing of the RB-MSS target rods due to thermal and irradiation effects was analyzed using ANSYS with a combined thermal-structural model. A thermal analysis of a single target rod was

performed to generate a temperature distribution in the cladding. This temperature distribution was imported into a static structural model to observe the effects of thermal strain on the cladding. The structural model was then adjusted to incorporate the effects of irradiation induced swelling by modifying the coefficient of thermal expansion of Zircaloy-4. Results of this analysis can be found in APPENDIX B of this report.

5.1.2.2 Diffuser

The diffuser has been made a direct subcomponent of the cartridge assembly to facilitate the handling and exchanging of the target rods. As part of the design, the cartridge and diffuser are intimately attached while down in the reactor position. In order to remove the cartridge, a lifting eye is machined to the diffuser assembly, subjecting the diffuser structure to hold the full weight of the cartridge and target rods. The full weight of the cartridge with 11 target rods is 17.95 lbs (8.16 kg) which yields a minimum design weight load of 80.05 Newtons that the Diffuser must be able to lift. A structural model was generated for the Diffuser weldment and the results are summarized in Section 7.2.2.3.1. The flow characteristics that the diffuser imparts on the cartridge exit flow are also detailed in 30441R00038.

5.2 Thermo- Hydraulics Summary

A full thermo-hydraulic analysis was performed to evaluate the flow needs of the target assembly as well as the pressure loads the Target Assembly will experience during normal operations and for accident scenarios such as loss of cooling. The full details on the thermo-hydraulics results can be found in 30441R00021.

6 ASSUMPTIONS

The following assumptions were used in the structural-mechanical analysis:

1. No strength reduction was assumed as a result of irradiation based on the effect of neutron irradiation analysis performed on GA Doc. No. 30441M00029.
2. There was no corrosion allowance for the design (preliminary test samples placed inside the MURR Pool only showed appropriate levels of oxidation). Images documented on email from Christopher Dohm titled "Corrosion Samples Monthly Update" sent on September 20, 2016, (Reference 8) of which a few sample images are appended to this document in APPENDIX A.
3. All TA components (except for the target rod components) are < 50°C, obtained from Doc. No. 30441R00021.
4. Materials of construction are as listed in Table 3.

Table 3: Materials of Construction

Parameter	Component	Material
Material of Construction	Upper Water Inlet Tube Section	UNS A96061
	Target Housing Weldment	UNS A96061
	Lower Housing Weldment	UNS S31603
	Cartridge Lower Flange	UNS A96061
	Cartridge	UNS A96061
	Lower Diffuser	UNS A96061
	Diffuser Outlet	UNS A96061
	Cladding	UNS R60804
	Upper Cladding Endcap	UNS R60804
	Lower Cladding Endcap	UNS R60804
	Cooling Line Flange	UNS A96061
	C-Seal	Inconel 718
	Pellets	95% Dense LEU, Y12 Standard Specification

5. The target assembly is expected to run and irradiate targets at most twice per week.
6. For the cladding, startups, shutdowns and changes in power are assumed to occur over a 0.05 day (1.2 hour) time period. Also, the extreme allowable conditions of the target rods are assumed for the analysis (i.e., the first and last day of a [redacted] irradiation is at 115% power). 5a, d, e, f
7. The total Cartridge pressure cycles are 104; based upon two cycles per week for a total of 1 year lifetime. No thermal cycles are assumed for the Cartridge.
8. The total Target Housing pressure cycles are 1,040; based upon two cycles per week for a total of 10 years. No thermal cycles are assumed for the Housing
9. Cladding cycles are based on a [redacted] operation 5a, d, e, f

7 STRUCTURAL ANALYSIS OF TARGET SYSTEM

7.1 Material Allowables

The allowable stress for AL6061-T6 and Stainless Steel 316L were obtained from Section II of the ASME B&PV Code (Reference 3), (Figure 16). These values will be used to evaluate safety and the limits of the Target Assembly components. Values for Zircalloy-4 were taken from Matweb (Reference 9) and in Table 4, a comparison is done to some of the material strength numbers as used by FRAPCON.

As a secondary check, Regulatory Guide 2.2, Reference 6, states:

a. *Regulatory Guide 2.2, Development of TS for Experiments in Research Reactors (referenced in NUREG-1573)*

Under Mechanical Stress Effects (C.1.c(3)):

Materials of construction and fabrication and assembly techniques utilized in experiments should be so specified and used that assurance is provided that no stress failure can occur at stresses twice those anticipated in the manipulation and conduct of the experiment or twice those which would occur as a result of unintended but credible changes of, or within, the experiment.)

To satisfy this condition, a minimum factor of safety of 2 will be applied to ensure no stress failure occurs in the Target Assembly components.

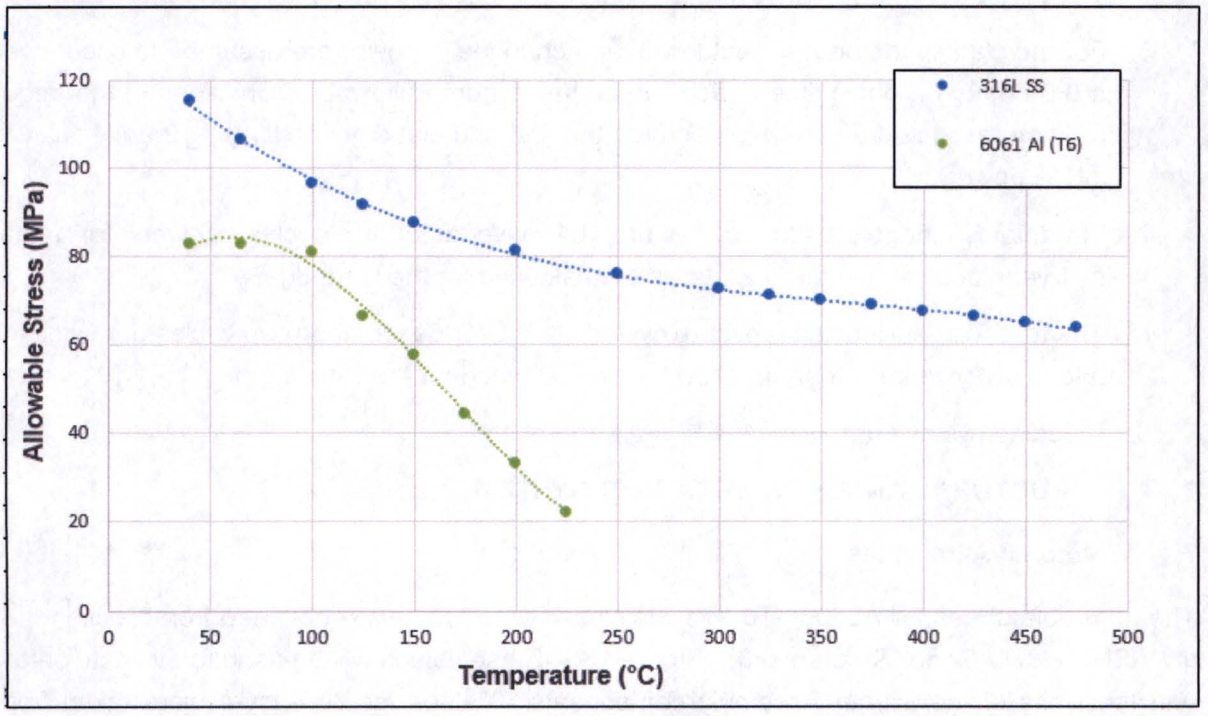

Figure 16: Allowable strength temperature Al 6061T6 and SST316L from ASME B&PV.

Table 4: Zircaloy - 4 Zirconium Alloy, UNS R60804 from MatWeb.com Vs FRAPCON

Physical Properties	Metric	English	Comments	FRAPCON
Density	6.56 g/cc	0.237 lb/in^3		6.52g/cc
Mechanical Properties	**Metric**	**English**	**Comments**	**FRAPCON**
Tensile Strength, Ultimate	>= 413 MPa	>= 59900 psi		
Tensile Strength, Yield	>= 241 MPa @Strain 0.200 %	>= 35000 psi @Strain 0.200 %		
Elongation at Break	20%	20%	in 50 mm	
Modulus of Elasticity	99.3 GPa	14400 ksi		81.5 GPa
Poissons Ratio	0.37	0.37		0.42
Shear Modulus	36.2 GPa	5250 ksi		30.2 GPa
Electrical Properties	**Metric**	**English**	**Comments**	**FRAPCON**
Electrical Resistivity	0.0000740 ohm-cm	0.0000740 ohm-cm		
Thermal Properties	**Metric**	**English**	**Comments**	**FRAPCON**
CTE, linear	6.00 µm/m-°C @Temperature 25.0 °C	3.33 µin/in-°F @Temperature 77.0 °F		
Specific Heat Capacity	0.285 J/g-°C	0.0681 BTU/lb-°F		
Thermal Conductivity	21.5 W/m-K	149 BTU-in/hr-ft^2-°F		
Melting Point	1850 °C	3360 °F		
Boiling Point	4375 °C	7907 °F		

Table 4: Zircaloy - 4 Zirconium Alloy, UNS R60804 from MatWeb.com Vs FRAPCON

Component Elements Properties	Metric	English	Comments	FRAPCON
Chromium, Cr	0.10%	0.10%		
Iron, Fe	0.20%	0.20%		
Oxygen, O	0.12%	0.12%		
Tin, Sn	1.40%	1.40%		
Zirconium, Zr	98.50%	98.50%		

7.2 Results

7.2.1 Target Housing

7.2.1.1 Housing Structural

A model was developed to evaluate the structural behavior of the housing assembly to ensure that the design can safely handle stresses when submitted to pressures that more than satisfy the nominal 100% and 115% flow conditions as outlined in Section 5. Taking the highest flow condition of 115% flow during the SCRAM of the reactor, the pressure the housing will see is calculated to be 17.42 psi [120.11 kPa] taken from Figure 15. Although it is not expected for the Housing to see pressures beyond the 17.42 psi [120.11 kPa], which occurs at 115% flow, the 21.5 psi [148.24 kPa] parameter is set as the design limit of the housing due to the stresses seen at the welds of the housing getting close to the stress allowables as defined in Figure 16 and with a knockdown factor applied due to the type of weld used.

At this 21.5 psi [148.24 kPa] pressure, the Target Housing performs very well as the maximum Von Mises stress generated is 8.75 ksi [60.317 MPa] localized at one of the corners of the Aluminum housing as seen in Figure 17a1 and 17c, and which is well within the allowable of 11.99 ksi [82.7 MPa] for AL6061 per Figure 16. The Von-Mises stresses for the SST316L housing components are below 5.80 ksi [40.00 MPa] as seen in Figure 17a2 for the most part on the main plenum body. There is a high point at a corner of the SST plate that reaches 8.39 ksi [57.815 MPa] as seen on Figure 17a2 but it is highly localized and still under the allowable of 24.95 ksi [172 MPa].

The linearized stresses at the high stress point of the housing, through the back wall and the side-plate weld location of the housing are shown in Figure 18. These stresses show a membrane plus bending value of 3.93 ksi [27.07 MPa], which is well below the 11.99 ksi

[82.7 MPa] ASME code allowable from Figure 16 and providing a factor of safety of 8.90 for the Housing when compared to the 34.95 ksi [241 MPa] yield for AL6061, more than satisfying NUREG 2.2 (Reference 6).

Per the guidelines from ASME Code Section III Div 1 Table UW-12 (Reference 10) type 3 weld, "single welded butt joint without the use of a backing strip" will be used on the welds for the housing. To satisfy the code, the weld joint cannot see stresses which are 60% of the allowables. Sixty percent of 82.7 MPa is 49.62 MPa or 7.20 ksi allowed at the weld location. The membrane plus bending stress at the weld is 3.93 ksi [27.07 MPa] which more than satisfies the limit outlined by Table UW-12 with the knockdown factor for the welding of the housing. This design limit is still very conservative as evidenced by the safety factor of 8.9 when compared to the yield for AL6061 on top of the 25.80% conservatism taken by designing to a higher pressure load.

The displacement generated by 21.5 psi [148.24 kPa] load is also small at 0.021 in [0.526mm] located at the center of the Housing and seen in Figure 17b. This slight expansion of the Housing does not cause it to interfere with the outer walls of the reactor nor touches the neighboring wedge, which retain a nominal spacing of 0.062 in [1.57mm] and thus poses no issue.

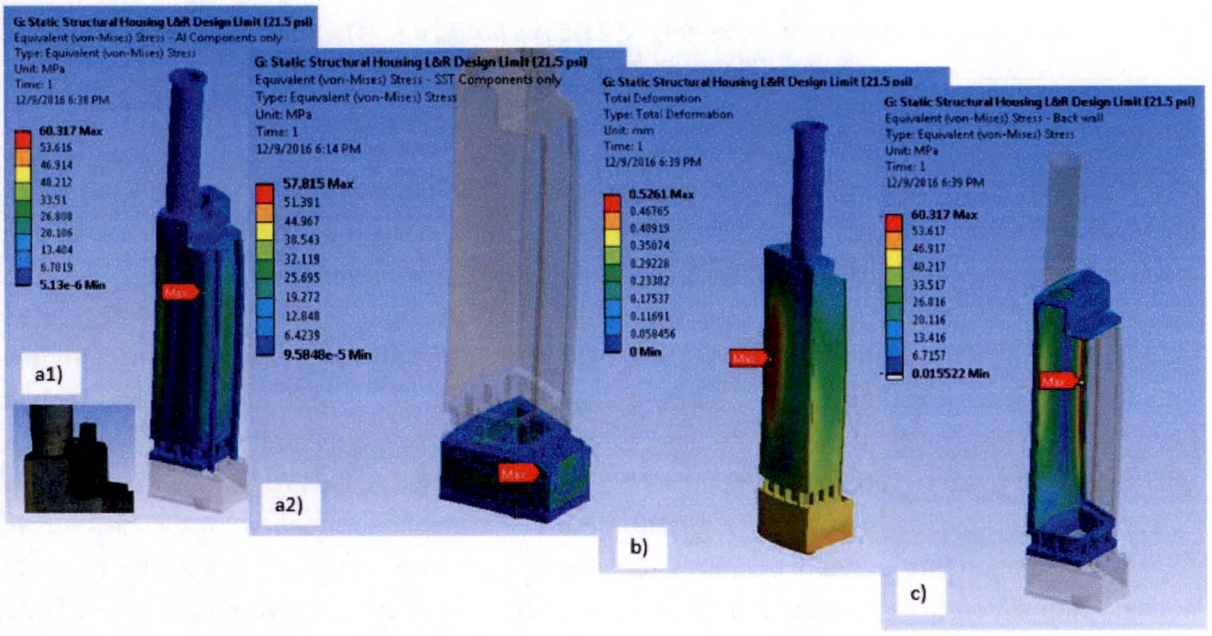

Figure 17. 21.5 psi design conditions model for the housing assembly, stresses and deflections

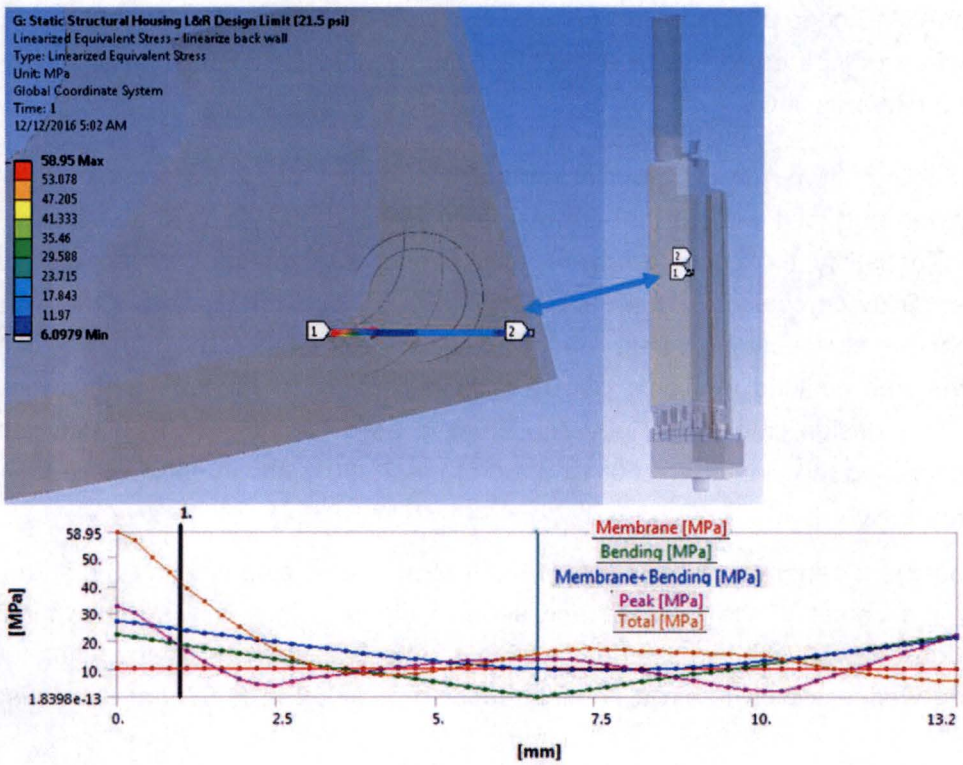

Figure 18. Linearized stress near corner for 21.5 psi [148.24 kPa] pressure design condition structural model for the housing assembly

7.2.1.2 Housing Fatigue

The Housing is designed to last a period of ten years. The highest number of expected cycles the housing will experience during that timeframe is ≤ 1,040 cycles based on current experiment plans that allow up to twice a week cycles. At the design pressure of 21.5 psi [148.24 kPa] for the housing, the primary stresses are well within yield strength of the SST316L (24.95 ksi [172 MPa] at 40°C) and for Al6061T6 (34.95 ksi [241 MPa] at 40°C). Also, due to the low amount of cycles and low primary stresses, pressure fatigue is not an issue as seen in Figure 19 and Figure 20 for both materials. Fatigue for steel does not start to become an issue until the cycles reach 100,000 as seen in Figure 19, and for Al6061T6, the stress levels of concern at 1000 cycles is at 27.56 ksi [190 MPa]. The highest stress point for the housing Aluminum components under 21.5 psi [148.24 kPa] loading is localized at the corner of the housing with a Von Mises stress of 8.75 ksi [60.317 MPa] (Figure 17a1) yielding a safety factor of 3.15. With the low number of cycles not being a concern, the yield value for SST316L is 24.95 ksi [172 MPa] and comparing this to the high point of stress for the SST316L components being 8.39 ksi [57.815 MPa] from Figure 17a2, a safety factor of 2.975 is achieved. Thermal fatigue is also not an issue for the housing as the expected thermal difference experienced by the housing will be only 10°C as compared to the pool temperature.

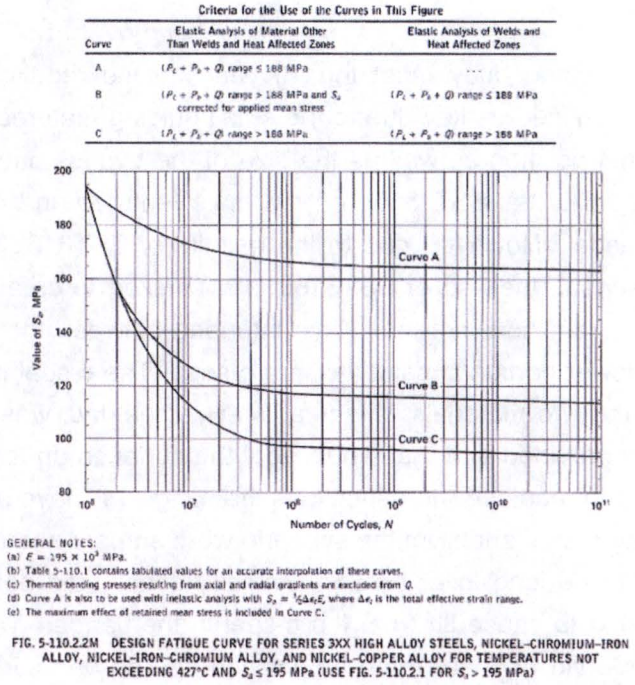

Criteria for the Use of the Curves in This Figure

Curve	Elastic Analysis of Material Other Than Welds and Heat Affected Zones	Elastic Analysis of Welds and Heat Affected Zones
A	$(P_L + P_b + Q)$ range ≤ 188 MPa	...
B	$(P_L + P_b + Q)$ range > 188 MPa and S_a corrected for applied mean stress	$(P_L + P_b + Q)$ range ≤ 188 MPa
C	$(P_L + P_b + Q)$ range > 188 MPa	$(P_L + P_b + Q)$ range > 188 MPa

GENERAL NOTES:
(a) $E = 195 \times 10^3$ MPa.
(b) Table 5-110.1 contains tabulated values for an accurate interpolation of these curves.
(c) Thermal bending stresses resulting from axial and radial gradients are excluded from Q.
(d) Curve A is also to be used with inelastic analysis with $S_a = \frac{1}{2}\Delta\varepsilon_t E$ where $\Delta\varepsilon_t$ is the total effective strain range.
(e) The maximum effect of retained mean stress is included in Curve C.

FIG. 5-110.2.2M DESIGN FATIGUE CURVE FOR SERIES 3XX HIGH ALLOY STEELS, NICKEL–CHROMIUM–IRON ALLOY, NICKEL–IRON–CHROMIUM ALLOY, AND NICKEL–COPPER ALLOY FOR TEMPERATURES NOT EXCEEDING 427°C AND $S_a \leq 195$ MPa (USE FIG. 5-110.2.1 FOR $S_a > 195$ MPa)

Figure 19. SST316L fatigue curve from ASME code (Reference 11)

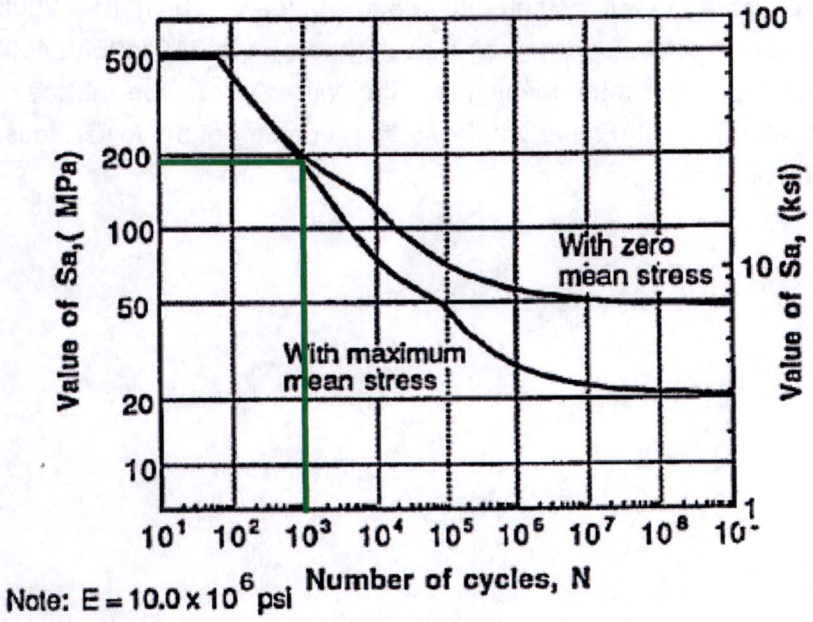

Figure 20. Aluminum 6061-T6 fatigue curve taken from "Fatigue Design Curves for 6061-T6 Aluminum" (Reference 12)

7.2.1.3 C-seal Analysis

In order to make the housing body meet the 10 year lifetime requirement, the cartridge to housing interface was identified as key due to the small guiding features that mount and install the cartridge into its final position as well as the size of the bypass prevention features. With this in mind, the decision to use SST 316L on the male features and Aluminum 6061 on the female features was made. However, due to the half-life of SST316L once activated and its associated cost for disposal, the use of SST316L is minimized to create an interface back to Aluminum 6061 for the main housing body. This interface between the aluminum body of the housing and the steel lower portion is sealed with a c-seal. The c-seal prevents water leakage and allows the use of the two materials. Manufacturer Jetseal Inc. was contacted to design a c-seal for the geometry provided and that would seal the surfaces up to 21.5 psi [148.24 kPa]. A model was generated to measure the deflections the flange will have under the load from the bolts compression of the c-seal and from the scenario were someone leans into the pipes at the top of the pool. Due to the long lever (~ 6.5m), small forces could potentially cause enough deflections in the housing to cause lift from the c-seal in the flange. The manufacturer has a recommendation of 250 lb/in of linear force around the seal to be used and that is what was loaded into the model.

To make sure this flange is stiff enough and the interface has no leakage due to deflections from the flange, an FEM was generated with the following loads: a) 21.5 psi [148.24 kPa] internal pressure with a 2000 lb/bolt preload [8896.44 Newtons/bolt], b) a 250lbs/in linear force on the c-seal groove (resistance from the c-seal), and c) a 21244 in*lbf [2400N*m] moment to simulate an average size man leaning on the water inlet pipe at the top of the pool (78.7lbs/35.7kg lateral load). Figure 21 shows the geometry of the lower housing flange with a 13-bolt configuration.

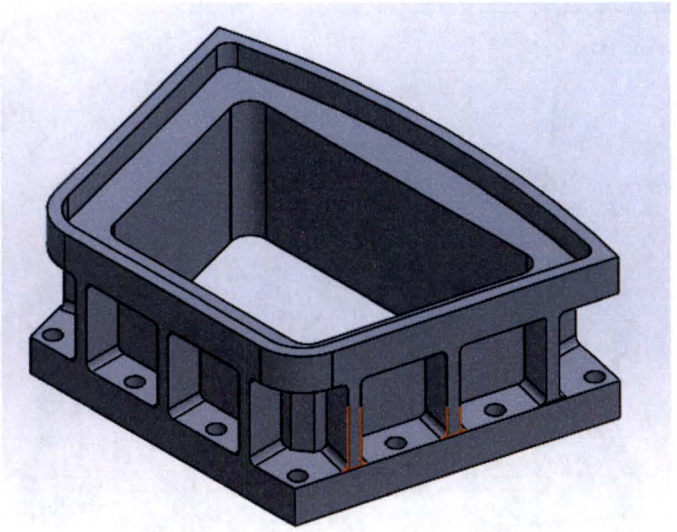

Figure 21. Geometry of the lower housing flange with a 13 bolt configuration

Figure 22 shows the deflections of the flange and the groove under the pressure and the moment loads. Deflections are minimal as expected due to the flange thickness of 0.75 inches in addition to the flange ribs providing a great amount of stiffness perpendicular to the mating flanges. The maximum deflection is 0.0065 inches [0.165mm] from point to point on the sealing surface of the groove under the load. The c-seal is designed with at least 0.013 inches [.3302 mm] elastic springback in order to prevent lift and avoid water bypass under these loading conditions and maintain a factor of safety of 2.

Although the 3" inlet pipe will be at ground level at top of the pool to avoid someone leaning on it, this extra level of robustness serves as margin for the expected loading of the design.

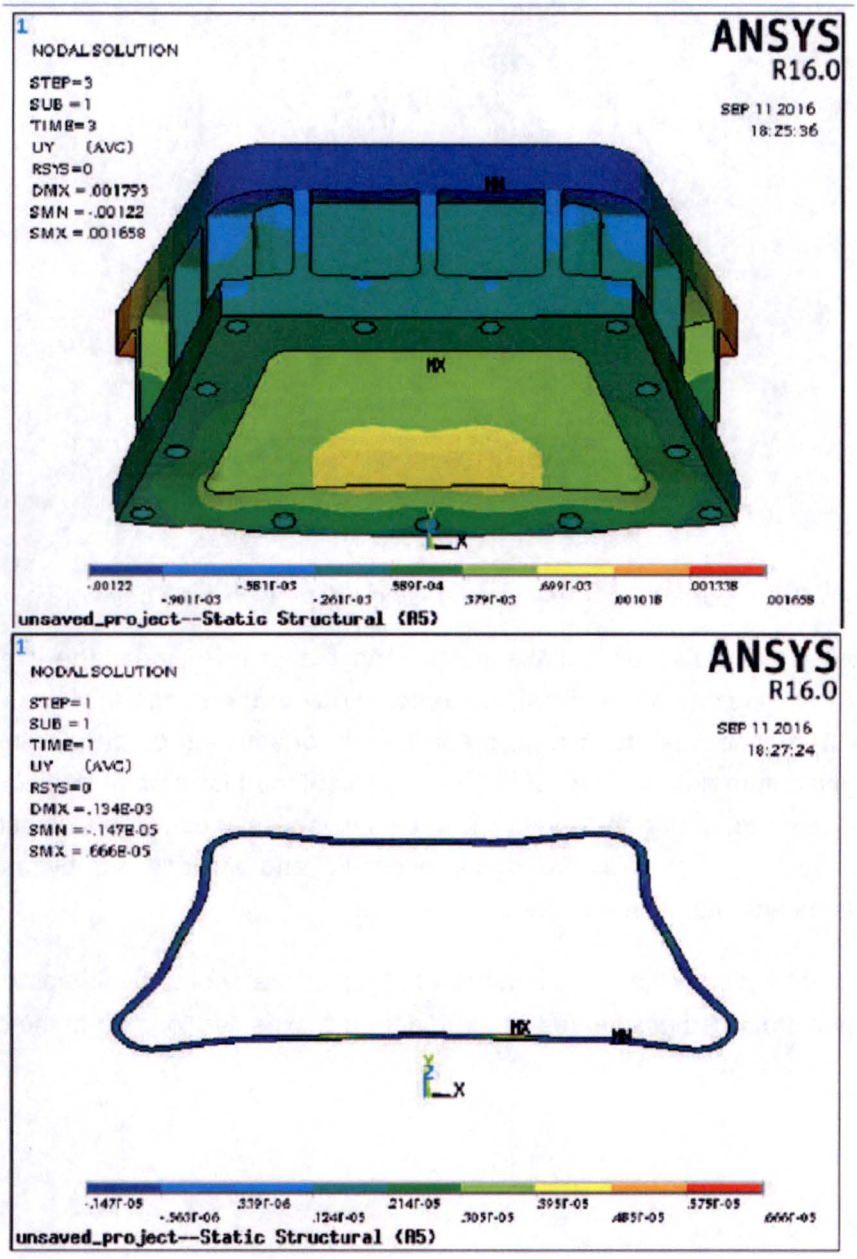

Figure 22. Deflections of the c-seal flange and groove under pressure and moment loads

As far as the stresses on the housing are concerned, Figure 23 shows the load of 2700N applied to the top of the housing. This is the equivalent of a 40kg/88.18lbs load being applied to the top of the line 22.47 feet [6.85m] above the housing, mimicking the weight of a person leaning on the pipe at the top of a pool and to show that the housing is more robust than the lift moment applied when analyzing the c-seal. Figure 23 shows the maximum Von Mises stress calculated from this load is 11.60 ksi [79.97 MPa] for one of the ribs on the lower flange and around 9.14 ksi [63 MPa] at the 3 inch inlet and top plate of the housing. Under these

conditions, having half the weight of an average person leaning on the pipe, the TA meets the allowable from the ASME code for AL6061 at 11.99 ksi [82.7 MPa]. It is the intention to institute procedures and administrative controls to not have a person lean on the pipes such as anchoring the pipe to a support structure at the top of the pool for support so that the support takes the load from someone accidentally leaning on the pipe but this analysis shows that the design can take a significant lateral load without damaging the housing.

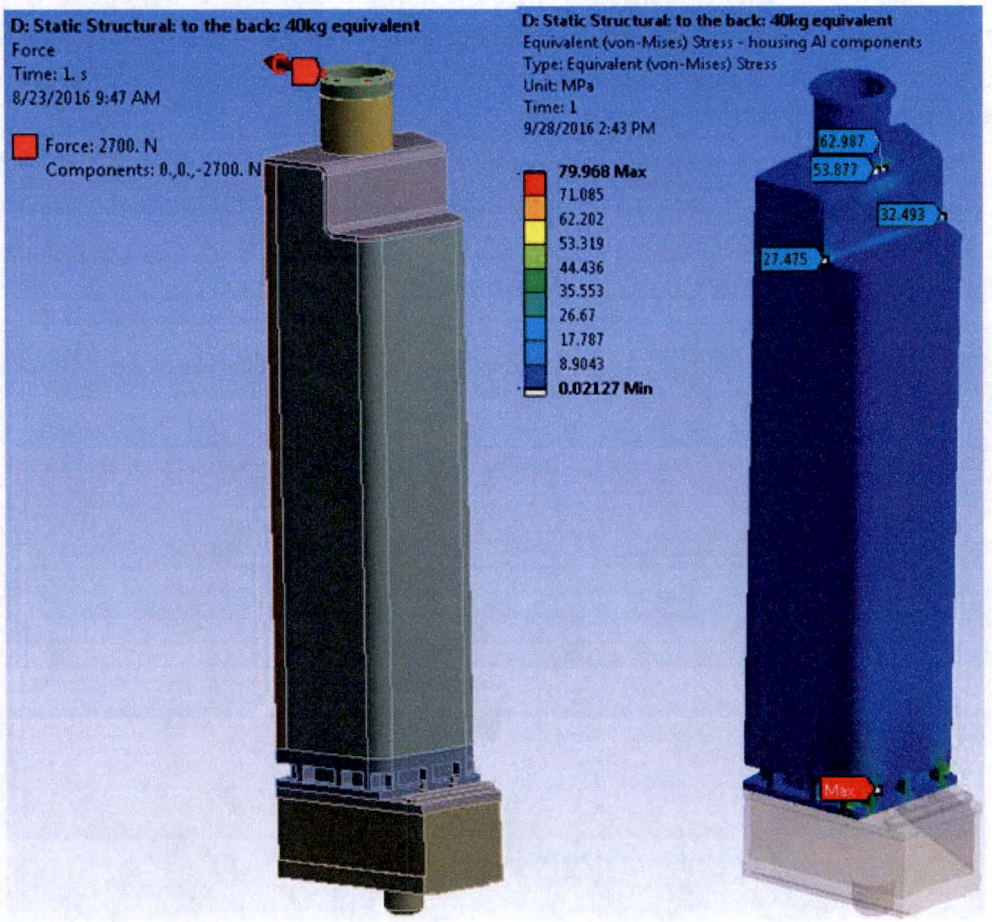

Figure 23. Radially outward load. 88.18lbs/40kg equivalent at top of pool

7.2.2 Cartridge Assembly

7.2.2.1 Cartridge

7.2.2.1.1 Cartridge Structural

A model was developed to evaluate the structural behavior of the cartridge assembly to ensure that the design can safely handle stresses when submitted to pressures corresponding to the nominal 100% and 115% flow conditions. Taking the highest flow condition of 115% flow during the SCRAM of the reactor, the pressure the cartridge will see is calculated to be 12.16 psi [83.84 kPa] taken from Figure 15. Although it is not expected for the cartridge to see pressures

beyond the 12.16 psi [83.84 kPa] which occurs at 115% flow, the 14.80 psi [102.04 kPa] load parameter is chosen as the design limit of the cartridge due to the stresses seen by the pins under the load and to maintain a minimum safety factor of 2 on those stresses to the yield of SST316L per the code.

The aluminum cartridge at the 14.80 psi [102.04 kPa] pressure fairs very well overall with the pins taking most of the load. Figure 24 shows most of the cartridge experiences very low Von Mises stress levels hoovering at 10.45-1.74 ksi [10-12 MPa]. The inside wall and small localized areas around the pins are the zones that see higher stresses. The cartridge sees total stresses up to 18.40 ksi [126.83 MPa] in highly localized areas around the pins but only 8.99 ksi [62.03 MPa] 1 mm deep into the cartridge main body as evidenced in Figure 25 when linearizing the stresses through the cartridge wall. At these locations around the pins, the membrane plus bending stresses through the cartridge wall of 8.45 ksi [58.25 MPa] as seen in Figure 25, show the design satisfies the ASME Code allowable of 11.99 ksi [82.7 MPa].

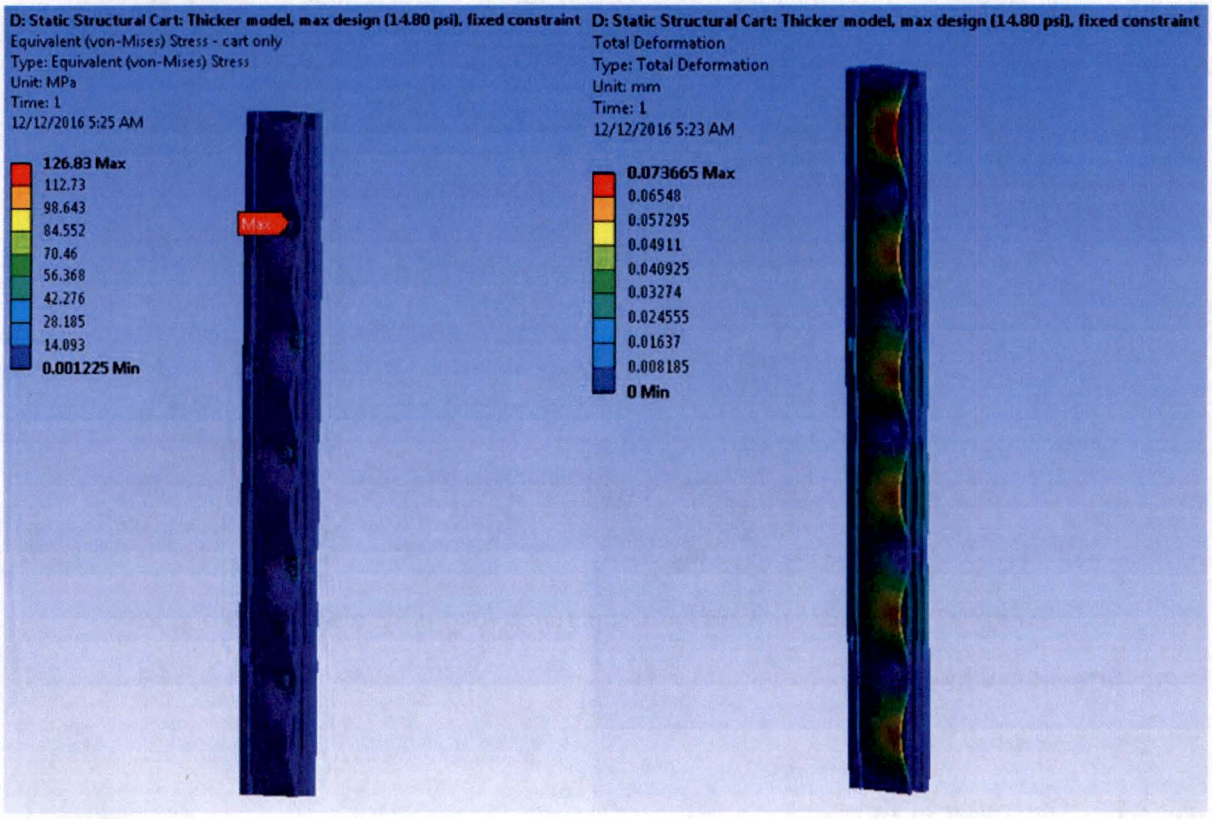

Figure 24. Cartridge at 14.80 psi design pressure condition. Stresses and deflections

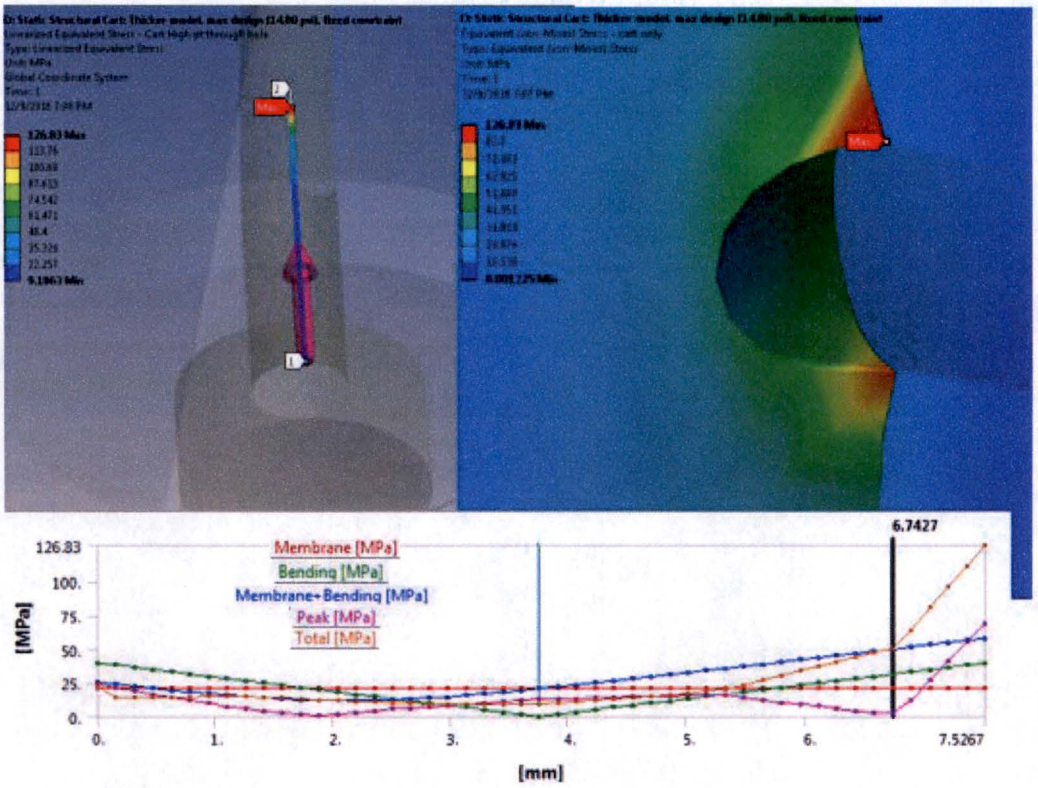

Figure 25. Cartridge at 14.80 psi design pressure condition. Linearized stress through cartridge wall

Figure 24 also shows the deflections under the 14.80 psi [102.04 kPa] load. The maximum calculated displacement of 73.7 microns occurs at top of the cartridge. The displacement generated by this pressure is small by design due to the placement of the pins which prevent large volumes of the cartridge body to balloon out, ensuring that the velocity from the cooling water around the target rods remains constant.

At the side walls, the cartridge see lower stresses than around the pins but just like in the Housing, and because the cartridge is fabricated as a clamshell halves, the strength at the weld seam must have a knockdown factor of 0.6. This brings down the allowable for AL6061 from 82.7 to 49.62 MPa or 7.20 ksi. As seen in Figure 26, the stresses at the inner surface have a high point of 6.36 ksi [43.88 MPa] but when linearized through the wall at this location, the membrane plus bending totals 2.98 ksi [20.55 MPa]. This satisfies the design welding limit due to the knockdown factor for the welding of the cartridge sides. In order to meet the ASME Code, the 14.80 psi [102.04 kPa] pressure is set as the limit for the design, due to the SST316L pins stresses and keeping a minimum factor of safety of 2 as shown in Figure 27.

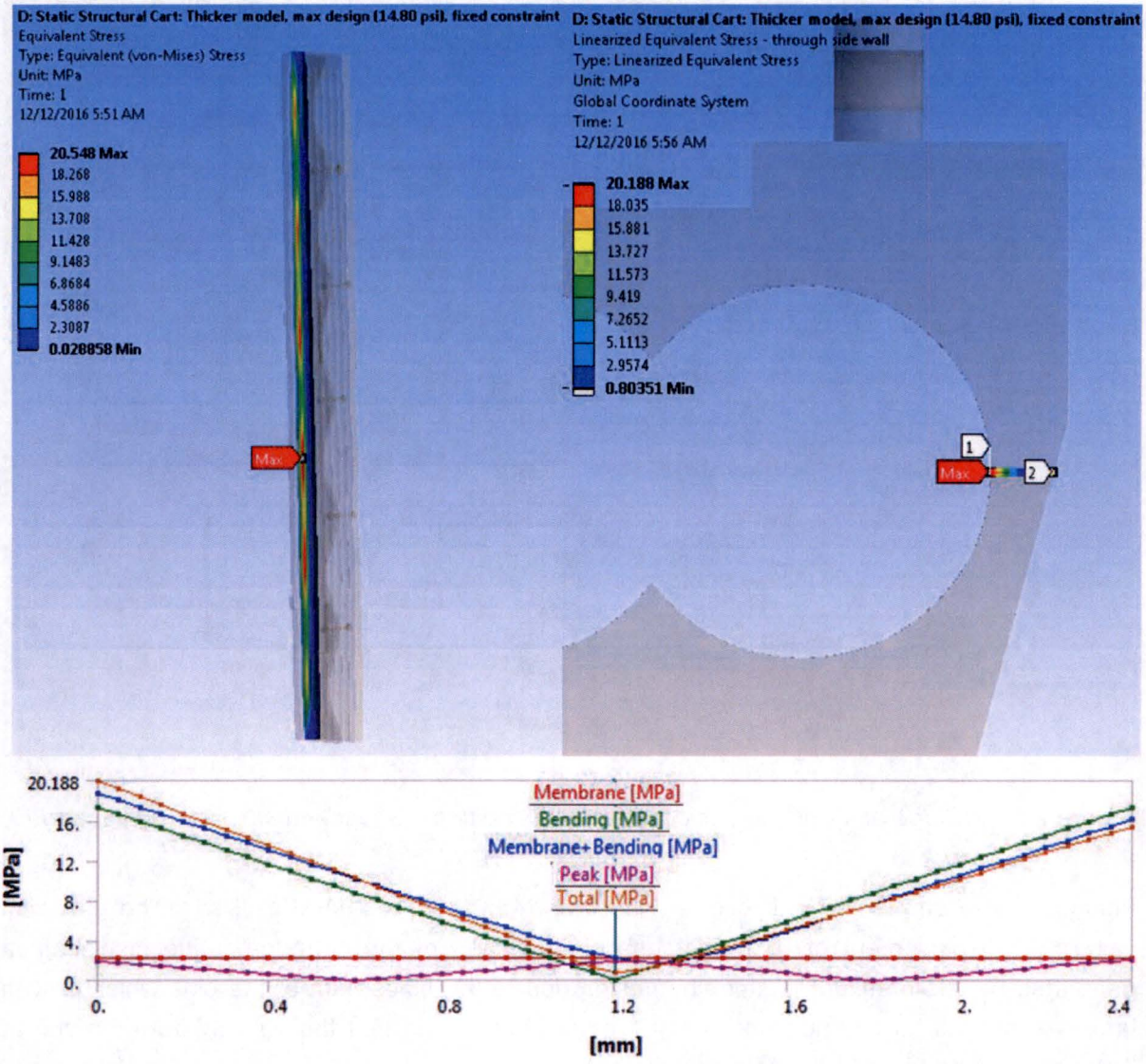

Figure 26. Linearized stresses of cartridge through at weld location for 14.80 psi loading conditions

As mentioned earlier, the pins by design are meant to take the brunt of the pressure load. Figure 27 shows that one of the pins sees a maximum Von Mises stress of 24.76 ksi [170.71 MPa] at the local point of contact and node shared with the cartridge's high point. As evidenced by the stresses on the rest of the pin and the linearization plot through the center of the pin it is clear that this high stress number is from the geometric discontinuity in the model of the cartridge coming to a point and meeting the pin. This is a self-limiting stress that does not affect the pin performance. When linearizing the stresses through the center of the pin, stresses of 13.89 ksi [95.83 MPa] are seen, but when broken down to the primary stresses

through the middle of the pin, the shaft only sees 8.66 ksi [59.71 MPa] when adding the membrane and bending stresses which are still below the 16.68 ksi [115 MPa] allowed.

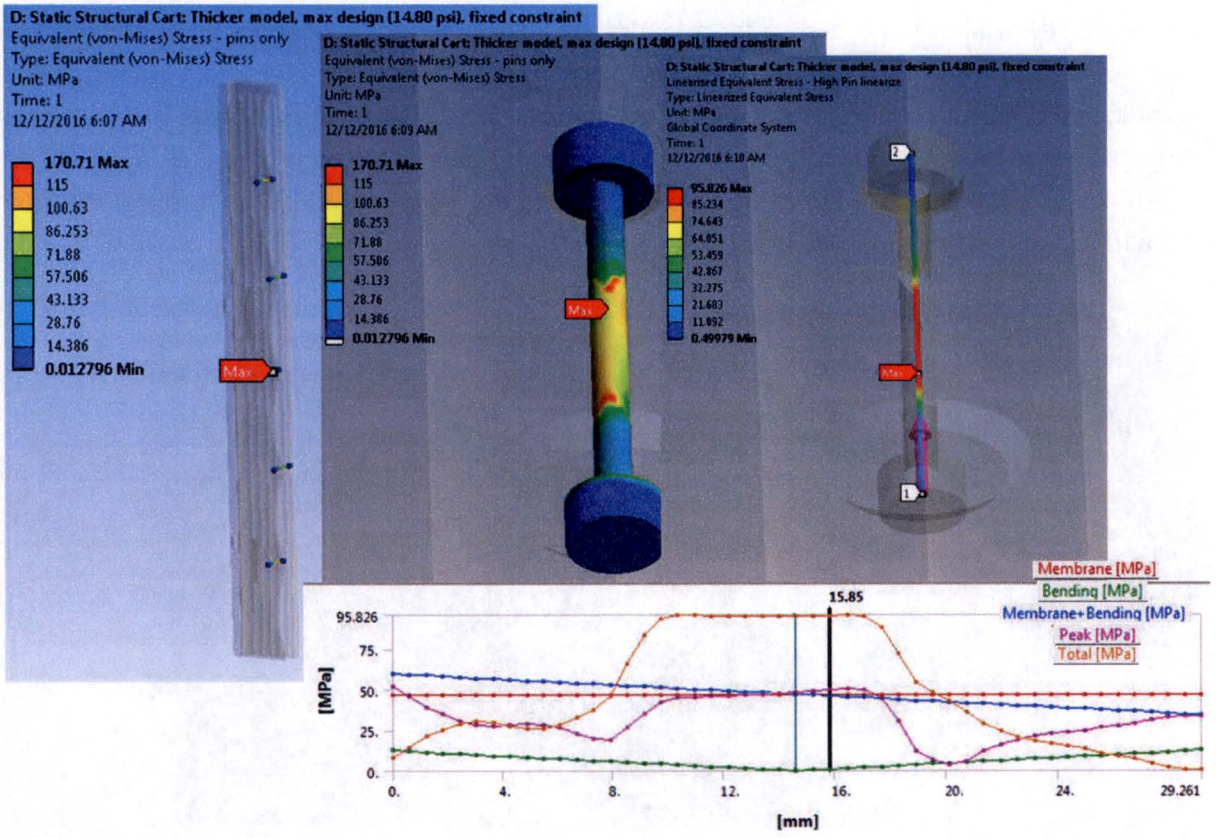

Figure 27. Cartridge at 14.80 psi design pressure condition. Pin maximum linearized stresses

The cartridge aluminum components maximum primary stress value is 8.45 ksi [58.25 MPa] as mentioned above in Figure 25. At this stress value, the cartridge aluminum parts have a 4.14 factor of safety when compared to the 34.95 ksi [241 MPa] yield for AL6061, more than satisfying NUREG 2.2. The SST316L pins see higher stresses as designed, with the highest pin seeing 8.66 ksi [59.71 MPa] primary stresses. The yield for SST316L is 24.95 ksi [172 MPa] per the already conservative ASME code which provides a 2.88 factor of safety to yield. However the 14.80 psi [102.04 kPa] load is already 21.7% higher than the highest expected value at 12.16 psi [83.84 kPa]. In order to maintain a minimum safety factor of 2 to yield and keep good margin in satisfying NUREG 2.2 (Reference 6), the loading of 14.80 psi [102.04 kPa] is set as the limit for the housing components. Although the NUREG 2.2 regulation states that the design must maintain a factor of safety minimum of 2 to failure, all of the design parameters for the target assembly are meeting this requirement to the yields of their materials for the extra margin.

Since the design pressure of 14.80 psi [102.04 kPa] for the cartridge shows the factor of safety to be over 2.88 to yield for the pins, and in order to have added margin, the 14.80 psi loading parameter was conservatively chosen as the maximum. This same model was calculated for the actual design pressure expected at the 115% SCRAM condition of 12.16 psi [83.84 kPa]. Figure 28 below shows the results for a loading of 12.16 psi [83.84 kPa] on the cartridge. The pins see a maximum localized stress 20.35 ksi [140.29 MPa] in the same pin-cartridge high point location as mentioned for the 14.80 psi loading case. When the stresses are linearized through the center of the shaft, the maximum bending plus membrane stresses are 7.12 ksi [49.07 MPa]. This yields a factor of safety of 3.51 to the yield of the SST316L allowable from the already conservative ASME code.

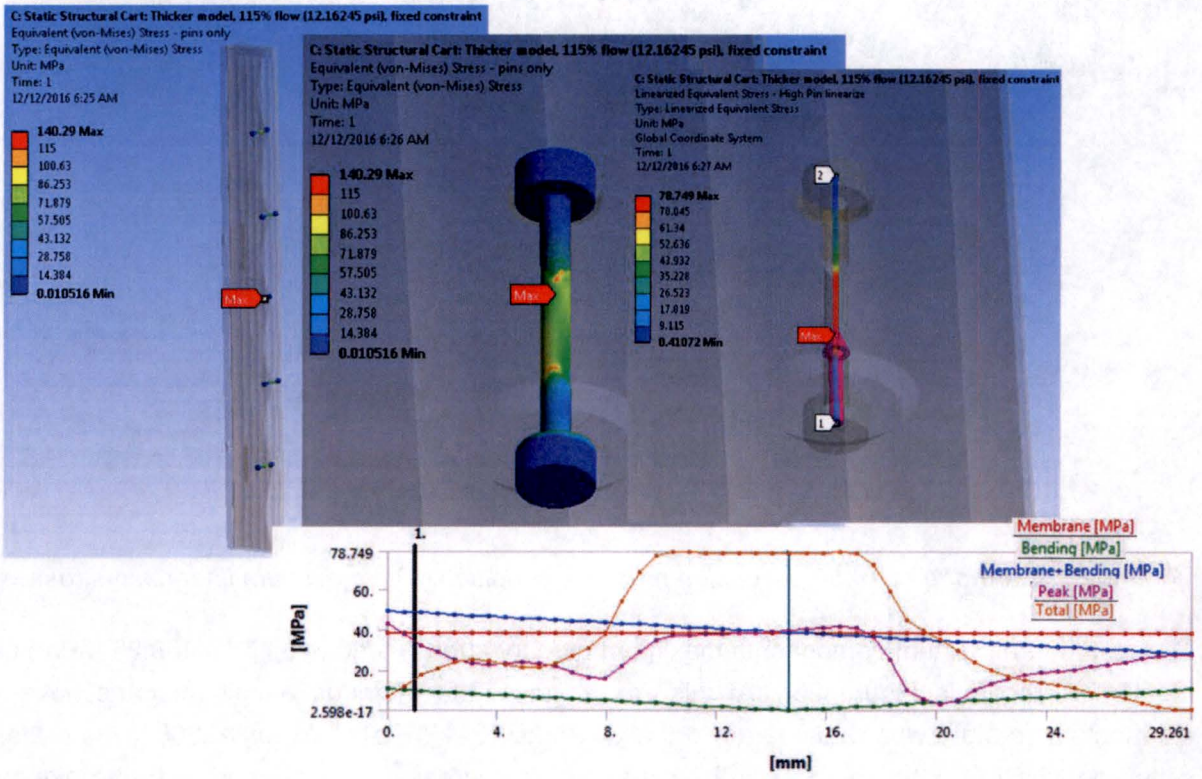

Figure 28. Cartridge at 12.16 psi design pressure condition (115% max flow). Pin maximum linearized stresses

7.2.2.1.2 Cartridge Fatigue

The cartridge is designed to last a period of one year. The highest number of expected cycles the housing will experience during that timeframe is < 104 cycles based on current experiment plans. At the design maximum design pressure of 14.80 psi [102.04 kPa] for the cartridge, the primary stresses are still within the code allowables and the yield strength for the SST316L (24.95 ksi [172MPa] at 40°C) and for Al6061T6 (34.95 ksi [241MPa] at 40°C) components. This gives the cartridge plenty of margin over the maximum expected stresses seen at the 115% flow

condition. Also due to the low amount of cycles, and low primary stresses, fatigue from the pressure load is not an issue as seen in Figure 19 for the stainless steel as it takes one million cycles before the onset of material fatigue and Figure 20 which sees the aluminum barely begin to see material fatigue at the expected 104 cycles. With the maximum aluminum stresses at 8.66 ksi [59.71 MPa] for the 14.80 psi [102.04 kPa] pressure case (from Figure 25), as seen in the curve from Figure 20 for this number of cycles, stress in not an issue. Thermal fatigue is also not an issue for the cartridge as the expected thermal difference experienced by the housing will be only 10°C.

7.2.2.1.3 Cooling Flow

7.2.2.1.3.1 Target water flow velocities

The coolant velocity distribution is important to ensure that all rods receive adequate convective heat removal. An ANSYS FLUENT (30441R00038) model was developed for the pinned cartridge design to evaluate the effect the pins would have in the water channel. The full details of the analysis are shown in 30441R00038, where the document shows that the flow has reached [redacted], and it is within [redacted] of the 5m/s target velocity a sixth of the way up the cartridge. From the contour plots, it is clear that the pins slow the flow down in the channels they reside in. However, in most cases the flow still remains above the [redacted] in all channels, and never drops below [redacted] ([redacted] below the target velocity). Given the margins calculated for the heat transfer and the localized nature of these velocity reductions, the simulation indicates that the flow distribution in over the target rods is sufficient to provide the necessary cooling.

5a, d, e, f

5a, d, e, f

7.2.2.1.3.2 Target water exit temperature and mixing

Another function of the diffuser is to mix the coolant flow exiting the 11 channels and provide a good thermal measurement of the water exiting into the pool. The design calls for an RTD to be inserted to the top of the diffuser to take this measurement. To evaluate that the shape of the diffuser does indeed provide adequate mixing, 30441R00038 shows the temperature contour plot that was created at the same elevation as the tip of the RTD sensor. Results show the coolant temperature around the RTD varies by less than [redacted], exhibiting sufficient mixing to accurately detect mixed mean coolant outlet temperature.

5a, d, e, f

7.2.2.2 Target Rods

7.2.2.2.1 FRAPCON Analysis

Pellet-clad interaction and the resulting stresses and strains on the cladding were analyzed using the computer code FRAPCON (References 13 and 14). FRAPCON-4.0 is the latest version of FRAPCON released September 2015. Patch 01 of FRAPCON-4.0 was released June 2016 and was used in all of the following calculations.

FRAPCON was developed by Pacific Northwest National Laboratory (PNNL) for the U.S. Nuclear Regulatory Commission (NRC) to calculate steady-state, thermal-mechanical behavior of light water reactor (LWR) oxide fuel rods. Phenomena modeled by the code include heat transfer through fuel and cladding to coolant, cladding elastic/plastic deformation, fuel-cladding mechanical interaction, fission gas release and rod internal pressure, and cladding oxidation. FRAPCON is used by the NRC as an independent audit tool in their review of LWR industry fuel performance codes. FRAPCON has been assessed against experimental data from 137 test cases (Reference 13).

Three analysis cases were examined with FRAPCON based on the gap size between the UO_2 pellet and the Zircaloy cladding: minimum gap of [redacted], nominal gap of 50 µm, and maximum gap of [redacted]. The three FRAPCON cases have the following file names with either *.inp for input, *.plot for plot file, or *.out for output. 5a, b, f

frapcon-[redacted]_100_115_3C
frapcon-50_100_115_3C
frapcon-[redacted]_100_115_3C

5a, b, f

These gap sizes are a result of allowable tolerances on the pellet outer diameter and cladding inner diameter. The geometric dimensions that define the FRAPCON analysis cases are presented below in Table 5.

Table 5: Geometric Dimensions Used in FRAPCON Analysis

	[redacted]	50 µm gap	[redacted]
Pellet outer diameter		5.000 mm	
Clad inner diameter		5.100 mm	
Clad thickness		0.500 mm	
Clad outer diameter		6.100 mm	
Scallop diameter		0.583 in.	
Pitch		0.458 in.	

5a, b, f

The specific target rod analyzed in FRAPCON is target rod 17 (from wedge 5B. See 30441R00031), which has the maximum power density and, therefore, the maximum local heat flux. FRAPCON uses an axial power distribution and a rod linear power to model the behavior of target rod 17 over a [redacted] irradiation period with mid-week and weekend shutdowns. In order to examine the target rod behavior at extreme allowable conditions, the first and last day of the [redacted] irradiation is at 115% power. At all other times the target is at 100% except for the shutdown periods when the target is generating decay heat from the buildup of fission products. The power history used in the FRAPCON analyses is shown in Table 6. 5a, d, e

[redacted]

Table 6: Power Histories Used in FRAPCON Analyses

Problem Time (days)	Problem Time (hours)	Linear Power (kW/m)
[redacted]	1.2	[redacted]
	24.0	
	25.2	
	48.0	
	73.9	
	75.1	
	78.0	
	79.2	
	96.0	
	120.0	
	151.9	
	153.1	
	168.0	
	169.2	
	192.0	
	216.0	
	241.9	
	243.1	
	246.0	
	247.2	
	264.0	
	288.0	
	319.9	
	321.1	
	336.0	
	337.2	
	360.0	
	384.0	
	409.9	
	411.1	
	414.0	
	415.2	
	432.0	
	456.0	
	462.7	
	463.9	
	487.9	

5a, d, e

5a, d, e, f

Startups, shutdowns, and changes in power are assumed to occur over a 0.05 day (1.2 hour) time period. Mid-week shutdowns begin with a 0.05 day (1.2 hour) power decrease to 0.0, a shutdown period of 0.12 day (2.9 hour), and end with a 0.05 day (1.2 hour) rise to full power. The weekend shutdowns have the shutdown period extended to 0.62 day (14.9 hour).

The linear rod power histories presented in Table 6 are based on a detailed MCNP6 analysis (30441R00032).

The axial power profiles used in the FRAPCON analyses are presented in Table 7. They are based on a detailed MCNP6 analysis which is then piecewise averaged to the 21 axial elevations used in the FRAPCON model. MCNP6 performance and validation for use in this calculation is detailed in 30441R00002.

Table 7: Axial Power Profile Used in FRAPCON

Elevation (m)	Axial Power Factor
0.00	0.952
0.03	1.060
0.06	1.148
0.09	1.214
0.12	1.258
0.15	1.282
0.18	1.307
0.21	1.280
0.24	1.259
0.27	1.227
0.30	1.186
0.33	1.133
0.36	1.069
0.39	0.993
0.42	0.904
0.45	0.804
0.48	0.695
0.51	0.586
0.54	0.489
0.57	0.423
0.60	0.418

RELAP5 Mod 3.3 Patch 03 was used to determine the steady state cladding temperatures at 100% and 115% power for all three FRAPCON cases (30441R00032). The six RELAP5 cases have the following file names with either *.inp for input or *.out for output.

1thruC_10.0MW_[redacted]SSnomF
1thruC_10.0MW_50SSnomF
1thruC_10.0MW_[redacted]SSnomF

1thruC_11.5MW_[redacted]SSnomF
1thruC_11.5MW_50SSnomF
1thruC_11.5MW_[redacted]SSnomF

5a, b, f

The cladding outer diameter temperatures are presented below in Table 8.

Table 8: Cladding Outer Diameter Temperature for Target Rod 17

	Cladding Outer Diameter Temperature at 100% Power (K)			Cladding Outer Diameter Temperature at 115% Power (K)			5a, b, f
Elevation (m)	[redacted]	50 µm gap	[redacted]	[redacted]	50 µm gap	[redacted]	
0.00	425.09	429.11	424.50	434.25	438.07	433.69	
0.03	430.06	433.90	429.50	438.65	442.49	438.09	
0.06	434.95	438.76	434.40	443.26	447.12	442.70	
0.09	438.79	442.63	438.23	447.00	450.88	446.43	
0.12	441.23	445.11	440.67	449.42	453.32	448.85	
0.15	442.33	446.23	441.76	450.53	454.44	449.96	
0.18	442.36	446.25	441.79	450.56	454.49	449.99	
0.21	441.65	445.51	441.08	449.84	453.77	449.27	
0.24	440.47	444.30	439.91	448.66	452.58	448.08	
0.27	438.97	442.77	438.41	447.17	451.08	446.60	
0.30	437.11	440.91	436.56	445.39	449.27	444.82	
0.33	434.70	438.50	434.14	443.11	446.96	442.55	
0.36	431.37	435.20	430.81	440.00	443.83	439.44	
0.39	426.71	430.57	426.14	435.64	439.44	435.07	
0.42	420.31	424.18	419.74	429.59	433.38	429.02	
0.45	411.95	415.79	411.38	421.58	425.37	421.02	
0.48	401.75	405.49	401.20	411.65	415.42	411.09	
0.51	390.43	393.96	389.91	400.38	404.07	399.83	
0.54	379.50	382.69	379.04	389.11	392.61	388.59	
0.57	371.60	374.30	371.22	380.24	383.34	379.77	
0.60	370.83	372.86	370.54	377.56	379.93	377.19	

Additional input parameters for FRAPCON are listed below in Table 9.

Table 9: Additional FRAPCON Input Parameters

Parameter	FRAPCON Input Value
Plenum length cold	3.9116 cm
Plenum spring outer diameter	0.4826 cm
Plenum spring wire diameter	0.635 mm
Plenum spring number of turns	17
Pellet dish depth	0.12 mm
Pellet end-dish shoulder width	0.55 mm
Chamfer height	0.08 mm
Chamber width	0.24 mm
Enrichment	19.75 %
Pellet apparent density	95.0%
Pellet surface roughness	1.0e-03 mm
Cladding cold work	0.40
Cladding surface roughness	1.0e-03 mm
Rod fill gas	95% He, 5% Air
Rod fill gas pressure	101325 Pa

FRAPCON results are presented below in four tables, Tables 10 through 13, for the time points in the power history of greatest interest: 0.05 day at 115% power, 1.05 day at 100% power,

[redacted] day at 100% power, and [redacted] day at 115% power. The results are either for the entire target rod or for axial node 6 out of 20 which has the peak power density and heat flux. 5a, d, e

Table 10: FRAPCON Results at 0.05 days at 115% Power 5a, b, f

	[redacted] gap	50 µm gap	[redacted] gap
Pellet centerline temperature (C)	2265	2331	2521
Pellet surface temperature (C)	389	422	533
Cladding ID temperature (C)	329	301	327
Cladding OD temperature (C)	177	181	177
Cladding average temperature (C)	253	241	252
Radial strain (%)	~~302~~	0.139	0.146
Axial strain (%)	0.053	0.104	0.109
Hoop strain (%)	0.212	0.138	0.146
Cladding internal pressure (MPa)	0.359	0.26	0.27
Cumulative fission gas release (%)	0.24	0.00	0.00
Cladding axial expansion (mm)	0.00	0.54	0.56
Fuel axial expansion (mm)	0.73 4.09	4.65	5.62

Table 11: FRAPCON Results at 1.05 days at 100% Power 5a, b, f

	[redacted] gap	50 µm gap	[redacted] gap
Pellet centerline temperature (C)	2011	2014	2196
Pellet surface temperature (C)	404	405	497
Cladding ID temperature (C)	302	279	301
Cladding OD temperature (C)	169	173	169
Cladding average temperature (C)	236	226	235
Radial strain (%)	-0.042	0.128	0.134
Axial strain (%)	0.155	0.098	0.102
Hoop strain (%)	0.259	0.128	0.134
Cladding internal pressure (MPa)	0.23	0.24	0.25
Cumulative fission gas release (%)	0.00	0.00	0.00
Cladding axial expansion (mm)	0.60	0.50	0.52
Fuel axial expansion (mm)	3.67	4.04	4.77

Table 12: FRAPCON Results at [redacted] days at 100% Power 5a, d, e

	[redacted] gap	50 µm gap	[redacted] gap
Pellet centerline temperature (C)	2161	2156	2278
Pellet surface temperature (C)	436	433	505
Cladding ID temperature (C)	302	279	301
Cladding OD temperature (C)	169	173	169
Cladding average temperature (C)	236	226	235
Radial strain (%)	-0.312	0.040	0.132
Axial strain (%)	0.273	0.141	0.102
Hoop strain (%)	0.485	0.202	0.137
Cladding internal pressure (MPa)	0.63	0.68	0.79
Cumulative fission gas release (%)	14.11	15.05	18.43
Cladding axial expansion (mm)	0.92	0.54	0.52
Fuel axial expansion (mm)	4.20	4.49	5.11

5a, b, f

[redacted]

5a, d, e

Table 13: FRAPCON Results at [redacted] days at 115% Power

	[redacted] gap	50 µm gap	[redacted] gap
Pellet centerline temperature (C)	2464	2450	2527
Pellet surface temperature (C)	447	438	489
Cladding ID temperature (C)	329	301	327
Cladding OD temperature (C)	177	181	177
Cladding average temperature (C)	253	241	252
Radial strain (%)	-0.664	-0.281	-0.011
Axial strain (%)	0.409	0.266	0.169
Hoop strain (%)	0.778	0.499	0.280
Cladding internal pressure (MPa)	0.72	0.78	0.92
Cumulative fission gas release (%)	15.19	16.07	19.46
Cladding axial expansion (mm)	1.36	0.84	0.64
Fuel axial expansion (mm)	4.70	4.98	5.65

5a, b, f

7.2.2.2.2 Pellet Clad Interaction Structural Evaluation Summary

As discussed in Section 7.2.2.2.1, "FRAPCON Analysis", the pellet – clad interaction for the target rods has been analyzed using FRAPCON 4.0 to ensure that the target performance does not exceed design limiting factors of fuel melting temperatures and cladding strain cycles. Each target rod, shown in detail in Section 3.2.3.2 nominally consists of 100, 95% dense UO_2 pellets that are encapsulated by the Zircaloy-4 cladding. Additionally, the Zircaloy-4 cladding was analyzed with 40% cold work after final annealing during manufacturing.

The pellets (see Figure 29) have been designed for optimum performance with manufacturability in mind. Dishing of both ends was added to minimize ratcheting effects in the cladding, while chamfers were added for ease of insertion and elimination of stress concentrations on the cladding from pellet rotation. The pellet to clad gap was optimized at [redacted] to minimize stress/strain in cladding on one hand and peak centerline temperatures on the other. When adding manufacturing tolerances, the gap varies between [redacted] and [redacted] microns. Additionally, the target rod void space is filled with > 95% He with the remainder air, at ≈1 atm, that aids the welding process and provides good heat transfer properties to minimize pellet centerline temperatures.

5a, b, f

5a, b, f

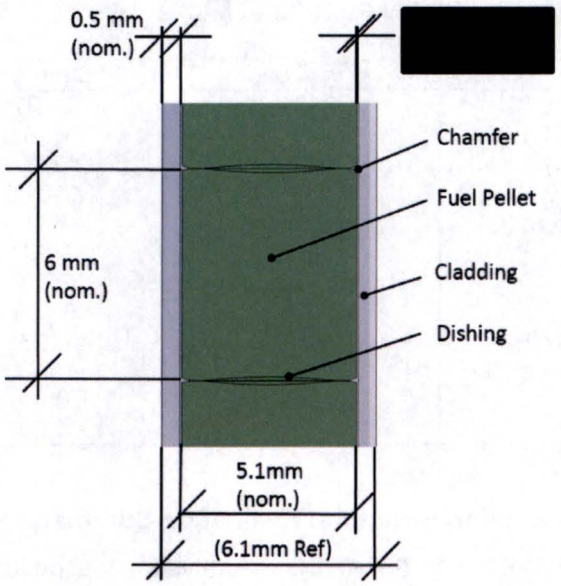

Figure 29. Pellet and cladding details

A nominal operational scenario suggests that depending on demand, the target cartridge could be pulled from the target housing any time between [redacted]. For analysis purposes therefore, it has been assumed that during the [redacted] period the reactor could see a maximum of 6 startups and shutdown cycles[redacted], though [redacted] cycles is more likely to be the nominal case if operated to the [redacted] limit. For analysis purposes it is assumed that at the beginning and end of the [redacted] period, the reactor would run at 115% (11.5 MWt) power for a period of 24 hours. At 115%, control rod run-in initiates and reactor SCRAM occurs at 125% (12.5 MWt). The result, an upsurge in fission gas release, internal pressure rise, and additional thermal growth and pellet relocation are experienced, though the duration and frequency is not enough to cause any design limit to be exceeded.

5a, d, e

The results of the FRAPCON analyses are shown in Table 14; extracted from Tables 10 thru 13 for cases of interest. Stresses and strains as a result of pellet-clad interaction are highest for the minimal cold gap ([redacted]). The results show that for the above operating/design conditions the primary pressure induced stress is 8.1 MPa, and well within the primary stress limit of Zircaloy-4 of 385 MPa (55840 psi), at temperature of 329°C (Figure 30). With a factor of safety of > 47 on primary stresses, the design meets ASME B&PV Code as well as Regulatory Guide 2.2 (C.1.c(3)) of the U.S. Atomic Energy Commission, (Reference 6), which requires factor of safety against failure of 2. Primary stresses are therefore not the driver for cladding failure. Secondary stresses as a result of thermal differential expansion and re-location of the cracked pellet on the other hand are the main drivers for longevity of the cladding. A yield strain for Zircaloy-4 at temperature of 0.778% is well within the strain range of twice of yield, 1.6%. This therefore meets the secondary stress intensity limit. With respect to cyclic fatigue for

5a, b, f

[redacted]

Zircaloy-4, Figure 31 [ASTM STP 1245 (Reference 15)], which includes irradiated specimens, shows that the maximum quantity of cycles that the cladding can sustain is 9,000. With only 6 expected cycles, the cladding has ample design margin.

Table 14: FRAPCON Results Summary

Temperature (°C)	[redacted] Gap	50 µm Gap	[redacted] Gap
Pellet centerline	2464	2450	2527
Pellet surface	447	438	533
Cladding ID	[redacted]	301	[redacted]
Cladding OD		181	
Cladding Average	253	241	252
Strain (%)			
Radial	-0.664	-0.281	0.146
Axial	0.409	0.266	0.169
Hoop	0.778	0.499	0.280
Gas Pressure (MPa)			
Cladding Internal	0.72	0.78	0.92

5a, b, f

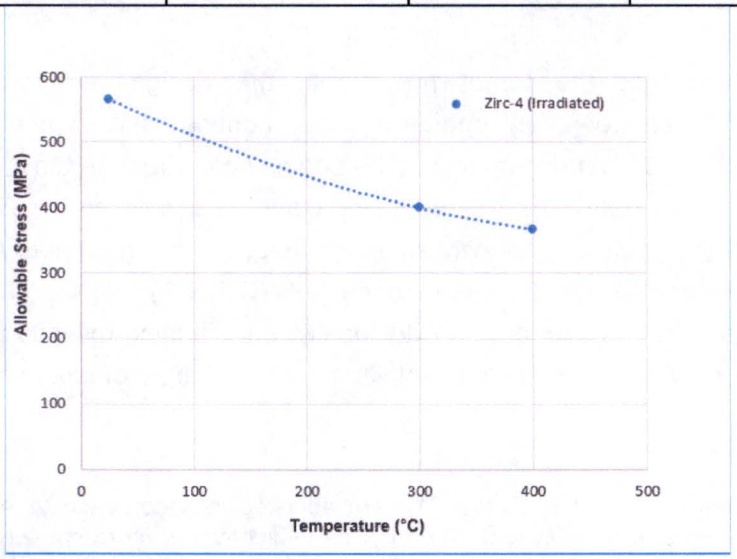

Figure 30. Allowable stress for Zircaloy-4 (irradiated) based on 2/3rd yield [Geelhood 2008 (Reference 15)]

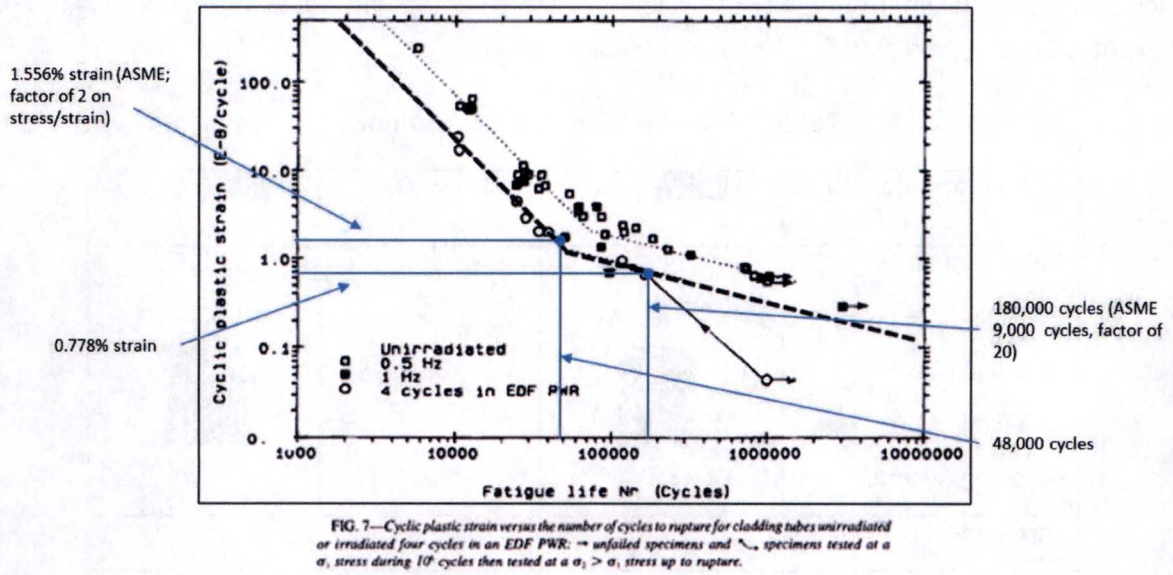

FIG. 7—*Cyclic plastic strain versus the number of cycles to rupture for cladding tubes unirradiated or irradiated four cycles in an EDF PWR:* → *unfailed specimens and* ↘, *specimens tested at a* σ_1 *stress during* 10^5 *cycles then tested at a* $\sigma_2 > \sigma_1$ *stress up to rupture.*

Figure 31. Fatigue chart Zircaloy-4, 350°C (unirradiated and irradiated) (Reference 16, 17, 18)[2]

In case of the maximum gap of [redacted], the upper limit of manufacturing tolerances, the concern is the centerline temperature of the target pellet. The maximum target pellet centerline temperature is 2527°C (Table 14). This value is well within the fuel melting temperature of 2840°C. 5a, b, f

The analyses show that the target rod meets the design requirements set forth in [30441S00001] and can be safely operated under nominal reactor conditions of 10 MWt, including the two (2) 11.5 MWt excursions at the beginning and end of the [redacted]. The design incorporates a safety factor of 1500 for cladding cycles and > 25000 for pressure-induced primary stress cycles. As previously mentioned, the design meets ASME B&PV Code, as well as Regulatory Guide 2.2 (Reference 6). (C.1.c(3)) of the U.S. Atomic Energy Commission with ample design margin. Additionally, the cladding exhibits a thermal margin of safety of > 140°C, while the target pellet exhibits a thermal margin of safety of > 313°C. 5a, d, e

---

[2] The reported values for cycles in Figure 31 were adjusted in accordance to ASME B&PV Code to provide a factor of 2 on stress/strain and 20 on cycles (whichever is more conservative). Per previous statement, with a factor of 2 on stress/strain, ASME B&PV covers the requirements of Regulatory Guide 2.2.This means that in case of 0.778% strain, applying a factor of 2, 1.556% strain, the quantity cycles are estimated at 48,000, or in case of 0.778%, using a reduction factor of 20, the expected cycles are 9,000 (180,000 cycles / 20). Note that these are adjustment factors to the experimental data set to obtain estimates of lives of components; per [NUREG/CR-6815 (Reference 17)].

7.2.2.2.3 Flow Induced Vibrations

According to the report ANL-GenIV-070 - Generation IV Nuclear Energy System Initiative Pin Core Subassembly Design, p. 57 (Reference 7): There are two primary concerns from the viewpoint of vibration analysis: i) the magnitude of turbulence-induced target rod displacements; (i.e., preclude rod-to-rod contacts which could result in damage accumulation over the course of plant operations), and ii) excitation mechanisms, wherein the frequency of flow field oscillations may match the natural vibration frequency of the rods, resulting in energy extraction from the flow field that can lead to target rod damage.

To address these two points, two different cases were calculated. In the two cases, the ends are tightly fixed so that they can support a moment in addition to being fixed in xyz directions. The variation for these two cases comes from having the rods be empty or tightly filled, where the rods are full (intimate contact with the cladding) and act to damp the vibrations.

For a 6.67 m/s axial flow speed in the cartridge channels, the flow induced vibrations are given in Table 15.

Table 15: Flow Induced Vibration Results

	Tightly Fixed Rods		
	Natural Frequency (Hertz)	**Displacement (Paidoussis) μm**	**Displacement (Blevins) μm**
Empty Rods	59.4629	6.0535	1.3665
Filled rods	47.292	1.0603	0.4221

Through machining tolerance, the minimum gap between the cladding and the pellets will be [redacted]. With such a close gap it is difficult to gauge how much the pellets do indeed act as a dampener so the empty case was evaluated first. Although the displacement will be smaller due to the mass of the pellets acting as a dampener, looking at the empty case the displacements through both, the Paidoussis and Blevins approach, the relative displacements are very small. At 6 microns, this magnitude of turbulence induced displacement does not pose a threat to the target rods and satisfying the first point from the ANL report (Reference 7) above. As for the second point, the report above also mentions "these types of instabilities are principally observed in situations involving cross-flow across tube banks". The cartridge single row design makes cross flow velocity components very small in the cartridge region as seen in Figure 10 of 30441R00038. In this figure, the lateral velocities are formed more as a result of the target rod being in the path of the flow more so than as a reflection of the cartridge design.

5a, b, f

[redacted]

At such small velocities and the natural frequencies calculated in Table 15, resonance effects from cross flow components are not an issue.

7.2.2.3 Diffuser

7.2.2.3.1 Weight Analysis

The cartridge assembly design details that the diffuser is an intimate component of the cartridge, so much so that the extraction procedure for the cartridge calls for the use of a feature on the diffuser to lift the cartridge assembly. This means the diffuser structure must be able to hold the weight of the cartridge assembly and the target rods within it, and not just be a ducting flow path for the water. An FEA model was created of the diffuser of which the models mesh is shown in Figure 32.

Each target rod has a mass of 0.366 lbs (0.166 kg) when filled with the pellets and there is a total of 11 target rods for a total mass of 4.02 lbs (1.83 kg). The target rod and the cartridge machined components masses are given in Table 16. Adding these together yields a total mass of 17.94 lbs (8.157 kg) so that the total load for the diffuser is 80 Newtons.

Table 16: Weight of Cartridge Components

Weight of Components		
	Pounds	**Kilograms**
Diffuser Ducting	0.84165	0.3825682
Diffuser lower flange	0.26086	0.1185727
Cartridge upper flange	0.20297	0.0922591
Cartridge Empty with pins	8.3023	3.7737727
[redacted]	[redacted]	[redacted]
Cartridge lower flange	0.8121	0.3691364
1x Target Rod with Pellets	0.3659	0.1663182
Total for Cartridge with 11 Target Rods filled with Pellets	**17.94648**	**8.1574909**

5a, b, d, e, f

Figure 33 shows the stress plot experienced by the diffuser taking the full weight load of 80 Newtons. The maximum Von Mises stress seen is 2.98 ksi [20.535 MPa] which is still well below (4.03 times) the allowable of 11.99 ksi [82.7 MPa].

[redacted]

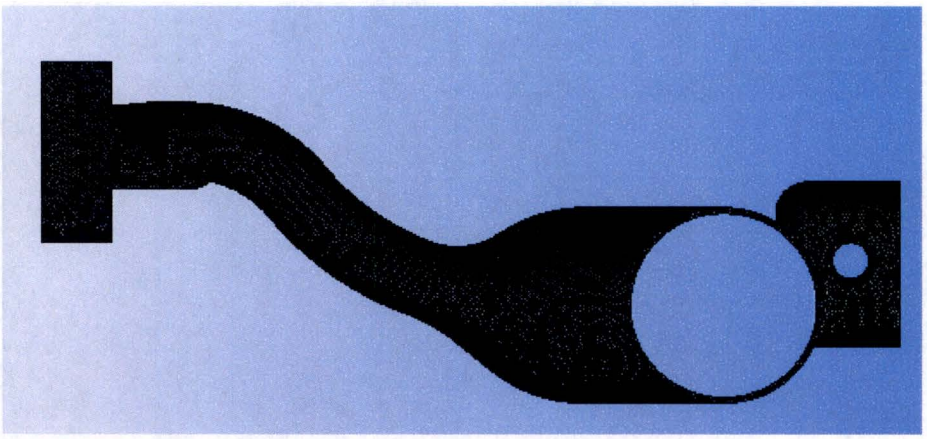

Figure 32. Diffuser weight analysis, meshing

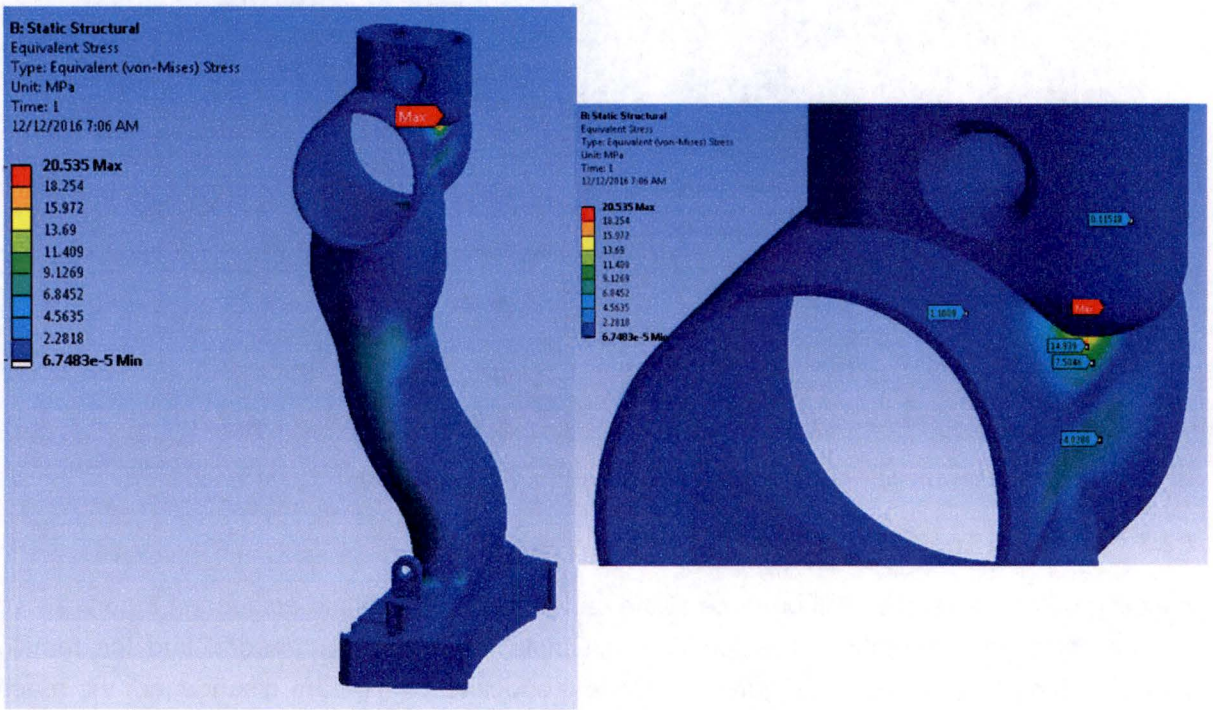

Figure 33. Diffuser weight analysis, stress results for 80N load

The pullout force limit for the diffuser is set by the max load the design can take before it begins to yield. Using the same model above, the stresses begin to reach the yield point of aluminum per the ASME code of 34.95 ksi [241MPa] (Figure 34) when the load reaches just over 940 Newtons. As a result, 850 Newtons is chosen as the maximum pull out force the diffuser assembly can take.

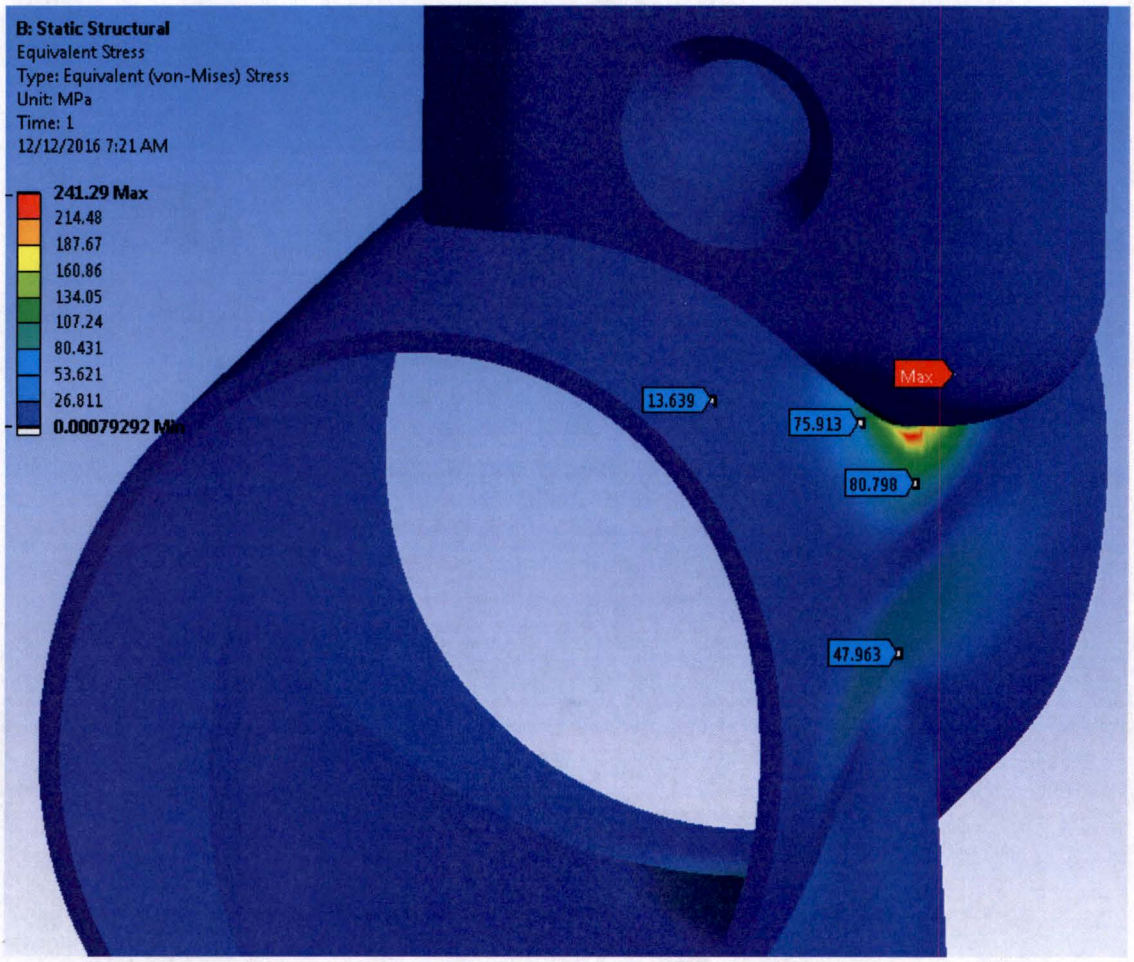

Figure 34. Diffuser weight analysis, stress results for 727N load

7.2.3 Handling Tools

Handling of the target rods will be done at the cartridge loading station as seen in Figure 2. To get the cartridge assembly to this location, a simple reach tool is threaded into the female cartridge lifting feature seen in Figure 35. Once the locking clamps are disengaged, the reach tool is threaded to the cartridge lifting feature which is at the center of mass of the cartridge assembly. As mentioned in Section 5.1.2.2 the total mass of a fully loaded cartridge assembly is 17.95 lbs (8.16 kg) so that the 3/8-16 thread from the lifting feature attached to a similarly 3/8 diameter reach tool is more than enough to lift the total combined anticipated weight of 26.4 lbs (12 kg) for the tool and cartridge. The anticipated stresses and deflections are minimal, in the order of 0.29-0.73 ksi [2-5 MPa] for this size reach tool and the weight of the cartridge assembly.

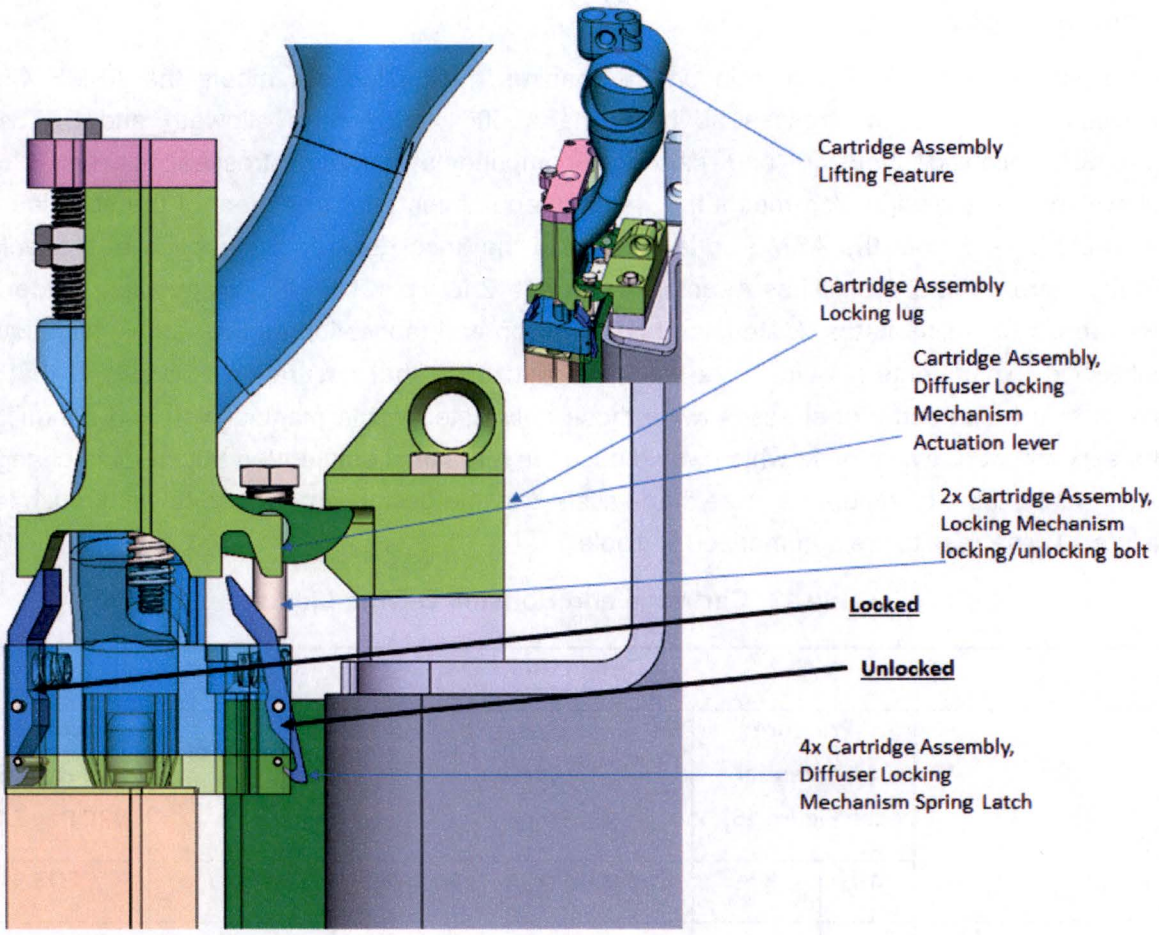

Figure 35. Cartridge assembly lifting and locking features

8 RESULTS SUMMARY

The structural analysis for the target assembly was performed in ANSYS Workbench R16. The calculations confirmed that the target housing and cartridge components are properly sized according to the ASME B&PV Section VIII, Division 1 and Section II-D, for normal and off-normal conditions. Based on this analysis, the structural design life of the target housing is conservatively estimated at 10 years while the design life of the cartridge is conservatively estimated for 1 year. The target housing and the cartridge, made from Al6061-T6 and Stainless Steel 316L, were analyzed for a maximum allowable design pressure of 21.5 psi (148.23 kPa) and 14.80 psi (102.04 kPa) differential respectively which gives an extra 21.7% margin on the design. The normal operating expected pressure for housing and cartridge (100% flow) will be 13.62 psi (93.91 kPa) and 9.63 psi (63.40 kPa) differential respectively. The flow conditions for which a SCRAM is initiated however (115% flow), increases the pressures the housing and

cartridge will see to 17.42 psi (120.11 kPa) for the Housing and 12.16 psi (83.84 kPa) to the cartridge respectively.

Even with an extra 21.7% margin on the loading, the design still meets the ASME Code allowables in terms of stresses as both, the AL6061 (82.7 MPa allowed) and SST316L (115 MPa allowed) housing and cartridge components primary stresses fall below the allowables. The design also meets the welding requirements for treatment of the stresses set by Table UW-12 from the ASME code, even with the knockdown factor applied at the welds. Furthermore, as the design has a factor of safety > 2 to yield, US NRC Regulation Guide 2.2 (Reference 6) which states "Materials of construction and fabrication and assembly techniques utilized in experiments should be so specified and used that assurance is provided that no stress failure can occur at stresses twice those anticipated in the manipulation and conduct of the experiment or twice those which would occur as a result of unintended but credible changes of, or within, the experiment" is more than satisfied as the design is not close to yield much less failure. These results are summarized in Table 17.

Table 17: Cartridge and Housing Design Limits

Design Limits						
	Pressure (differential, see Figure 15)		Lifetime		Max Pool Temperature	Factor of Safety (US NRC Reg 2.2)
	psi	kPa	Cycles (Max)	Years (Max)	Centigrade	FOS
Target Assembly Housing plus Cartridge	18	124.1	N/A	N/A	N/A	N/A
Housing	21.5	148.2	1040	10	50^0	8.90
Cartridge	14.80	102.04	104	1	50^0	2.88

The stresses for the cladding and pellet interaction similarly are found to be low when compared to the allowed. Stresses and strains as a result of pellet-clad interaction are highest for the minimal cold gap ([redacted]). The results show that for the above operating/design conditions the primary pressure induced stress is < 8.1 MPa, and well within the primary stress limit of Zircaloy-4 of 55840 psi (385 MPa), at temperature (Figure 30). Secondary stresses as a result of thermal differential expansion and re-location of the cracked pellet where identified as the main drivers for longevity of the cladding. A yield strain for Zircaloy-4 at temperature of 0.778% is well within the strain range of twice of yield, 1.6%. This therefore meets the secondary stress

5a, b, f

[redacted]

intensity limit. With respect to cyclic fatigue for Zircaloy-4, Figure 31 [ASTM STP 1245 (Reference 15)], which includes irradiated specimens, shows that the maximum quantity of cycles that the cladding can sustain is 9,000. With only [redacted] expected cycles, the cladding has ample design margin. With a factor of safety of > 47 on primary stresses, and an expected lifetime of [redacted] cycles out of 9000 cycles limit on the secondary stresses, the design meets ASME B&PV Code as well as Regulatory Guide 2.2.

5a, d, e

The performance of the diffuser as a means to extract the cartridge was also analyzed and found to be more than capable of lifting the weight load of a fully loaded cartridge (80N Weight). The maximum pull out force of 850 Newtons was also conservatively calculated based on the maximum Von Mises stresses under this load.

Based on the results of the analysis presented in this report, the maximum differential pressure for the Target Assembly shall not exceed 18.0 psi [124.1 kPa] at the inlet of the Target Assembly under any operating conditions, so as not to exceed the cartridge pressure of 14.80 psi, which is the limiting component pressure.

9 REFERENCES

1. ASME Boiler and Pressure Vessel Code Section VIII, Division 1, 2015.
2. ASME Boiler and Pressure Vessel Code Section VIII, Division 2, 2015.
3. ASME Boiler and Pressure Vessel Code Section II, Parts A Thru D, Material Specifications, 2015.
4. ASME Boiler and Pressure Vessel Code Section IX, 2015.
5. ASME Boiler and Pressure Vessel Code Section V, 2015.
6. Regulatory Guide 2.2, Development of Technical Specifications for Experiments in Research Reactors, U.S. Atomic Energy Commission, November 1973, under mechanical stress effects (C.1.c(3)).
7. Farmer M. T., Hoffman E. A., Pfeiffer P. F., Therios I. U., Wei T. Y. C. "ANL-GenIV-070 - Generation IV Nuclear Energy System Initiative Pin Core Subassembly Design", 2006.
8. Dohm, Christopher email "Corrosion Samples Monthly Update" sent on Sept. 20, 2016 to Katherine Murray, Junaid Razvi, Chad Carnavale & Hoai Dovan. (APPENDIX A).
9. Zircalloy-4 material properties retrieved from MATWEB from http://www.matweb.com/search/DataSheet.aspx?MatGUID=e36a9590eb5945de94d89a35097b7faa&ckck=1
10. ASME Boiler and Pressure Vessel Code Section III, Division 1.
11. ASME. VIII, Division 2 Alternative Rules, Rules for Construction of Pressure Vessels. New York: ASME, 2004

12. Fatigue Design Curves for 6061-T6 Aluminum", G.T. Yahr, Engineering Technology Division Oak Ridge National Laboratory, 1993.

13. Geelhood, K. J., et al., "FRAPCON-4-0: A Computer Code for the Calculation of Steady-State, Thermal-Mechanical Behavior of Oxide Fuel Rods for High Burnup," PNNL-19418, Vol. 1, Rev. 2, September 2015.

14. Geelhood, K. J., et al., "FRAPCON-4-0: Integral Assessment," PNNL-19418, Vol. 2, Rev. 2, September 2015.

15. Geelhood, K. J., Luscher, W. G., and Beyer, C. E., "PNNL Stress/Strain Correlation for Zircaloy," PNNL-17700, Pacific Northwest National Laboratory, July 2008.

16. Garde A.M., Bradley E.R., ASTM STP 1245 "Zirconium in the Nuclear Industry: Tenth International Symposium: 1994.

17. NUREG/CR-6815, Review of the Margins for ASME Code Fatigue Design Curve – Effects of surface Roughness and Material Variability, Argonne National Laboratory, September 2003.

18. Roark, Raymond J., Formulas For Stress and Strain, fourth edition, McGraw-Hill Book Company, New York, 1965.ASME. II, Part A Ferrous Material Specifications (Beginning to SA-450), Materials. New York: ASME, 2011a Addenda.

APPENDIX A - CHRIS DOHM EMAIL AND SELECTED REPRESENTATIVE IMAGES

Chris Dohm Email and Selected Representative Images

Dovan, Hoai

From: Dohm, Christopher C. <dohmc@missouri.edu>
Sent: Tuesday, September 20, 2016 9:25 AM
To: Carnevale, Chad
Cc: Dovan, Hoai; Razvi, Junaid; Murray, Katherine
Subject: -EXT-FW: GA Corrosion Samples Monthly Update
Attachments: S1-A (1).JPG; S1-A (2).JPG; S3-A (1).JPG; S3-A (2).JPG; S4-A Back side (1).JPG; S4-A Back side (2).JPG; S4-A Background and S2-A Foreground (1).JPG; S4-A Background and S2-A Foreground (2).JPG; S4-A Front Side.JPG; B Sample Rig.JPG; S1-B (1).JPG; S1-B (2).JPG; S2-B Foreground and S4 - B Other side background (1).JPG; S2-B Foreground and S4 - B Other side background (2).JPG; S2-B Foreground and S4 - B Other side background (3).JPG; S3-B (1).JPG; S3-B (2).JPG; S3-B (3).JPG; S4-B (1).JPG; S4-B (2).JPG; S4-B.JPG; S1-C (1).JPG; S1-C (2).JPG; S1-C (3).JPG; S1-C (4).JPG; S2-C Foreground and S3-C Background.JPG; S2-C Foreground and S4-C Other side Background (1).JPG; S2-C Foreground and S4-C Other side Background (2).JPG; S2-C Foreground and S4-C Other side Background (3).JPG; S2-C Foreground and S4-C Other side Background (4).JPG; S2-C Foreground and S4-C Other side Background (5).JPG; S4-C (1).JPG; S4-C (2).JPG; S4-C (3).JPG

Hi Chad,

Forwarding the attached images per Les' request below....

Chris

From: Foyto, Leslie P.
Sent: Tuesday, September 20, 2016 11:18 AM
To: Dohm, Christopher C.
Cc: Brooks, Kenneth W.
Subject: GA Corrosion Samples Monthly Update

Chris,
Please send to GA.
Thanks,
Les

Chad,
We pulled the GA Corrosion Samples on Monday, September 19th, and documented their condition with the attached pictures (time stamp is wrong). Please let me know if you have any questions.
Note: The dark to blackish color is definitely an oxide layer. We did not wipe off with a rag.
Thanks,
Les

1

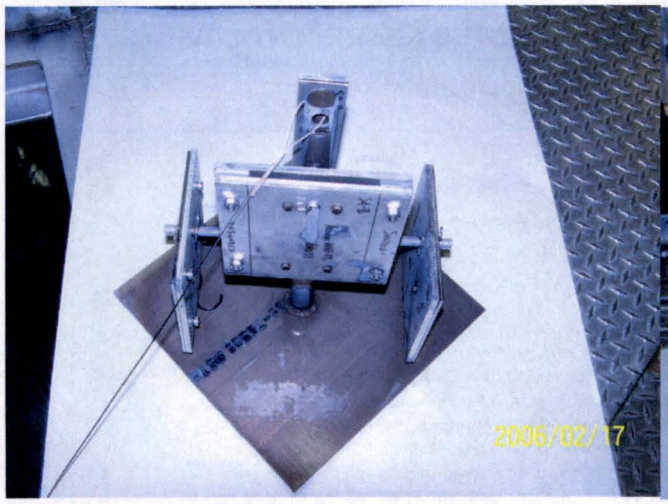
2006/02/17

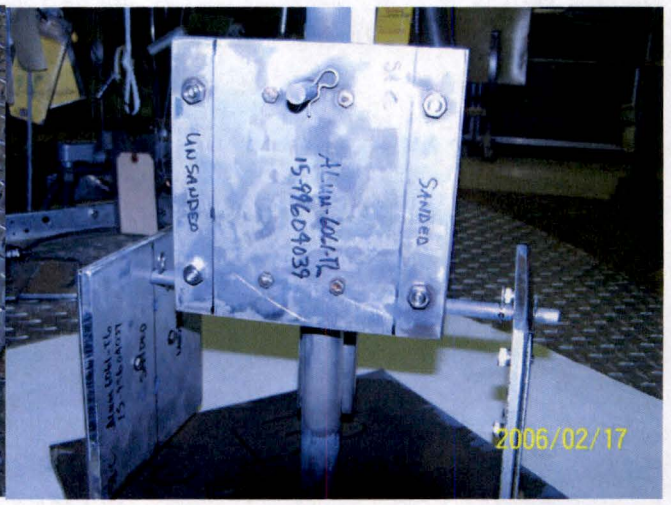
UNSANDED
SANDED
2006/02/17


SANDED
UNSANDED
2006/02/17


UNSANDED
2006/02/17

APPENDIX B – TARGET ROD BOWING DUE TO THERMAL AND IRRADIATION EFFECTS FOR SGE EXPERIMENTAL FACILITY

Material Properties

Material properties for UO_2 (pellet stack) and Zircaloy-4 (cladding and end caps) were taken from the IAEA's *Thermophysical properties database of materials for light water reactors and heavy water reactors* [1]. Aluminum 6061-T6 properties (bottom support grid) were taken from the ASME pressure vessel code [2].

Thermal Model

The thermal model of the single target model rod included the cladding tube with both end caps, a holder at the bottom end cap to approximate the bottom support grid, and a solid internal cylinder representing the UO_2 pellet stack. To incorporate the non-uniformity of the heat generation, this pellet stack cylinder was split into equal front and back portions. The model also utilized a symmetry plane through the axis of the target rod and perpendicular to the target stack split to reduce computation time. The model is illustrated in Figure 36.

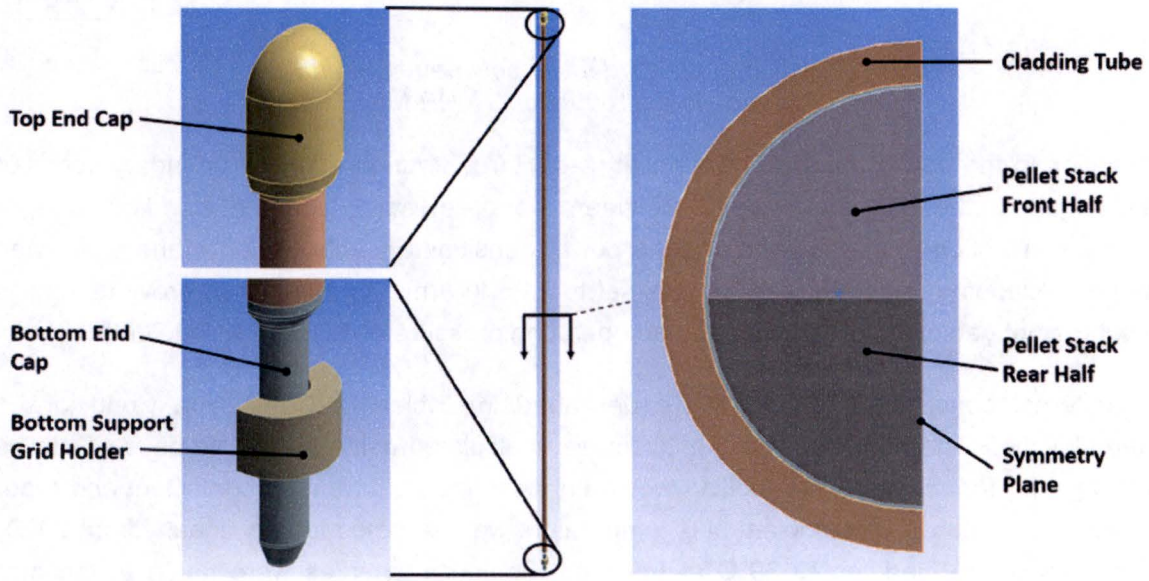

Figure 36. 3D geometry for target rod bowing analysis.

Data for the front-to-back power skew was taken from GA's MCNP model of the RB-MSS in the MURR pool [30441R00031]. The ratio of the power density between the front and back of the UO_2 pellet stack was captured for each rod at 50 axial nodes. The data for this power skew displayed as a scatter plot in Figure 37. Rods 1 through 11 and Rods 12-22 come from the two separate RB-MSS assemblies. The plot shows that there is considerable variation in the power skew, both from rod to rod and within each rod itself. Rod 9, which had the highest average skew of all rods, was highlight to show this variation.

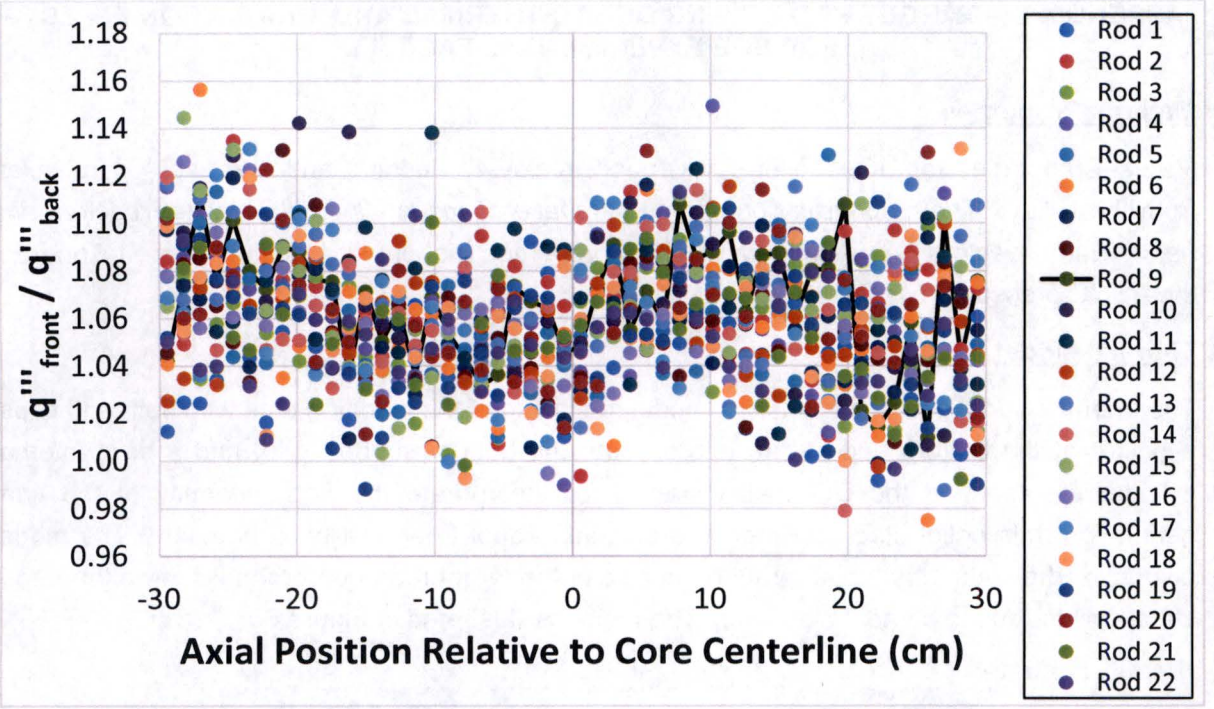

Figure 37. Ratio of power density between front and back of UO_2 pellets throughout GA RB-MSS

In addition to the power density in the pellet stack, three boundary further boundary conditions were required: the gap conductance between the pellet stack and the cladding tube, the external convection to the coolant, and the power densities of each section of the pellet stack. The pellet-cladding gap conductance was set to 21.5 kW/(m²*°C), based on previous analysis showing a **hot gap width of 10.3 µm and an operating pressure of 1.7 bar** [30441R00021].

The external convection conditions are described in Table 18: Convection Conditions for External Tube. The heat transfer coefficient was calculated using the single-phase Gnielinski correlation [3] for conservatism (boiling would enhance the heat transfer coefficient and reduce the wall temperature). The coolant bulk temperature was assumed to vary linearly from 29°C at the bottom of the cladding to 39°C at the top. Coolant properties were taken at the mean temperature of 34°C.

Table 18: Convection Conditions for External Tube

Coolant velocity, m/s	5.0
Density, kg/m^3	994.4
Coolant viscosity, Pa*s	0.000743
Coolant thermal conductivity, W/m*K	0.621
Cartridge hydramulic diameter, mm	10.0
Reynolds number	67,030
Prandtl nummber	4.99
Friction factor	0.0202
Nusselt number	374.5
Heat transfer coefficient, W/(m^2*°C)	23,270

The power density distribution was analyzed for two cases. In the average case, the power density of the front half of the pellet stack is assumed to be 6% greater than the rear half. In the worst case, the power density of the front half is assumed to be 16% greater than the rear half. This worst case assumption is extremely conservative, as only a few points throughout both targets come close to this power skew, and the average skew for rods containing those points is much lower. For additional conservatism, for both cases the entire stack was assumed to have the maximum power density of 57.25 kW/m, or 2,916 W/cm^3. The front-rear breakdown for both cases is given in Table 19: Power Density Variation in Pellet Stack for Average and Worst Case.

Table 19: Power Density Variation in Pellet Stack for Average and Worst Case

	Average distribution	Worst case distribution
Front half power density, W/cm^3	3,001	3,132
Rear half power density, W/cm^3	2,831	2,700

Results – Thermal

Figure 38 shows the radial temperature profile of the target rod across the axial midpoint for the rod with the worst case power skew. The power distribution is tilted toward the negative radial position. As the graph shows, this does move the peak temperature slightly away from pellet centerline, but only by about 0.17 mm. The tilt in the temperature profile causes a temperature difference in the cladding from front to back. Based on radial averages of the cladding temperature at the front and the back, the temperature difference between these two locations is about 16.8°C. The average temperature change from the cold condition is 190-210°C.

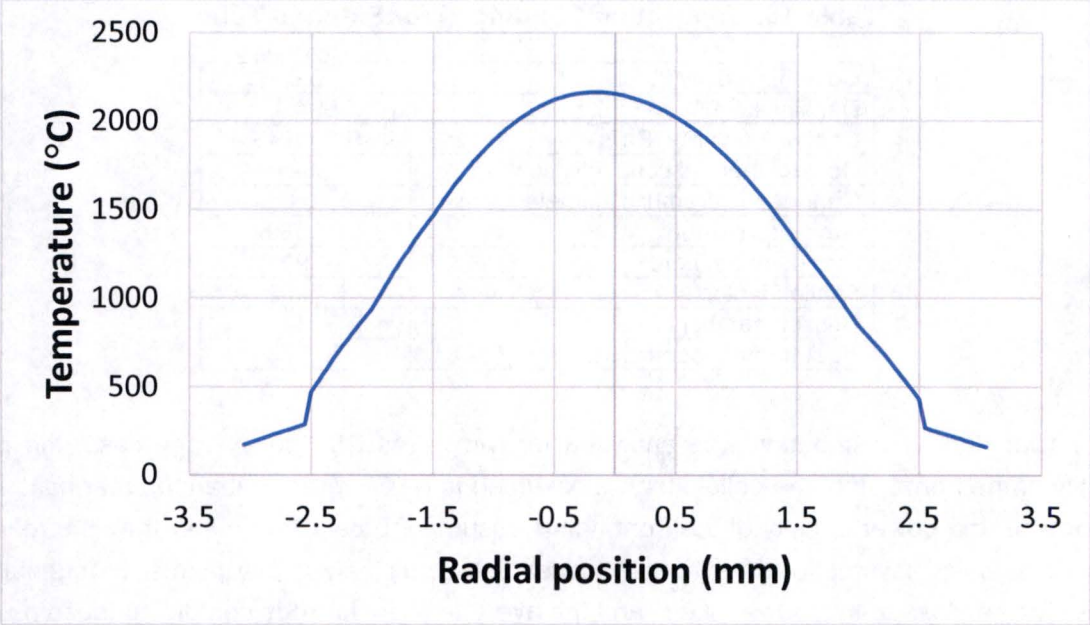

Figure 38. Radial temperature profile of target rod for worst case power skew

Structural Model

The structural model uses the same 3D geometry as the thermal model, except that the pellet stack has been removed. As the pellets were only necessary to generate the correct cladding temperature distribution, and do not provide any structural support to the cladding rod, this has no effect on the structural simulation.

The structural model requires three boundary conditions: a fixed support on the top end cap, the imported temperature profile from the thermal simulation, and a contact condition for the bottom end cap and the bottom support grid holder. The outer surface of the extended diameter portion of the top end cap can be treated as fixed because it is effectively constrained by the upper support grid. The imported temperature profile generates the precise thermal strain field that causes the bowing due to the front-to-back power skew.

The final condition, the contact setting between the bottom end cap and the bottom support grid holder, is required because there is a small radial gap of about 0.1 mm between the two components. The contact condition allows the end cap to deflect until it hits the inner surface of the support grid holder, at which point it becomes constrained. This contact was considered frictionless, as most contact force should be in the normal direction.

Adjustment for Irradiation

An initial analysis was performed of the thermal effects on cladding growth, using the worst case front-to-back power density skew. The resulting deformation showed an axial growth of the cladding rod of approximately 0.65 mm. This result is shown in Figure 39, where the black outline shows the undeformed position of the bottom end cap of the target rod. Output from FRAPCON analysis [30441R00032] showed that the irradiation growth of the cladding rod was 0.56 mm. Therefore, it was deemed that the effects of the irradiation induced growth could be captured conservatively by in the model by using doubling the Zircaloy-4 coefficient of thermal expansion in the structural model. This is a reasonable assumption because the irradiation strains are induced by fast neutrons, which come primarily from the UO_2 pellets contained in the target rods (neutrons from the MURR core are well thermalized by the time they reach the target). Therefore, the front-to-back asymmetry of neutron flux in the cladding rod should follow the asymmetry in the temperature distribution.

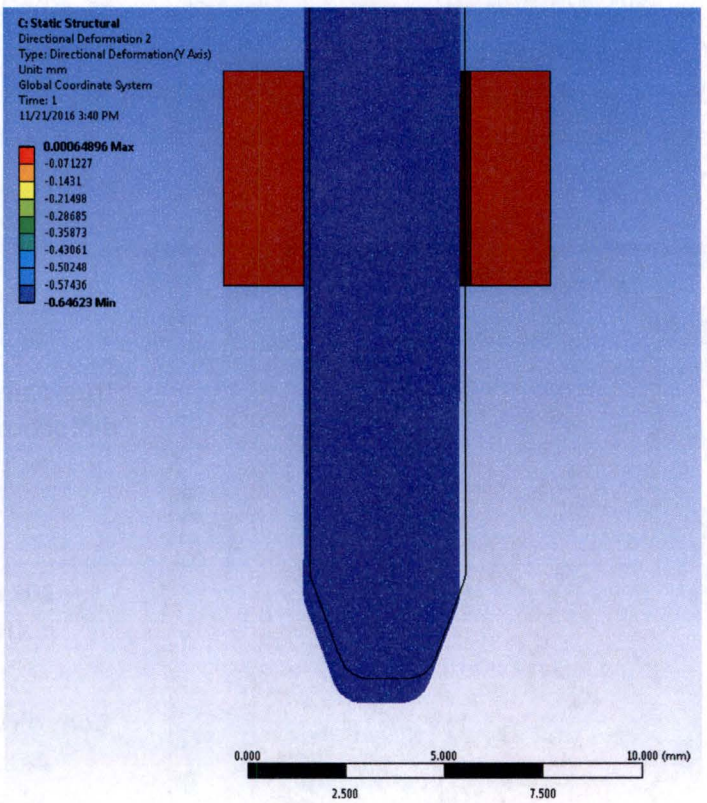

Figure 39. Thermal deformation in axial direction of RB-MSS target rod end cap

Results – Structural

The structural simulations were run for both average and worst-case power skews. The results show that the temperature differential between the front and back of the cladding causes the

bottom of the cladding rod to deflect away from the MURR core until the bottom end cap hits the back face of the inside of the bottom support grid. This deflection can be seen above in Figure 39. The contact between the end cap and the bottom support grid causes the middle of the target rod to deflect forward. It is the forward deflection near the axial center of the rod where displacement is highest. The results for the deflection are given in Table 20.

Table 20: Power Density Variation in Pellet Stack for Average and Worst Case

Case	Maximum Horizontal Deflection, mm
Average front-to-back power skew	0.060
Worst-case front-to-back power skew	0.607

Figure 40 provides a visual depiction of deflection of the target rod for the very conservative worst-case power skew. The figure shows the black wireframe of the un-deformed geometry, with the deformed body colored according to the deflection. The left portion of the figure shows a 1:1 scale of the deflection at its worst point, which shows the maximum deflection of 0.61 mm as slightly greater than the thickness of the cladding (0.5 mm). The right portion of the figure shows the overall deflection of the target rod by magnifying the displacement by a factor of 30. This greatly exaggerated bowing makes it easier to visualize how the power skew causes the target rod to deform.

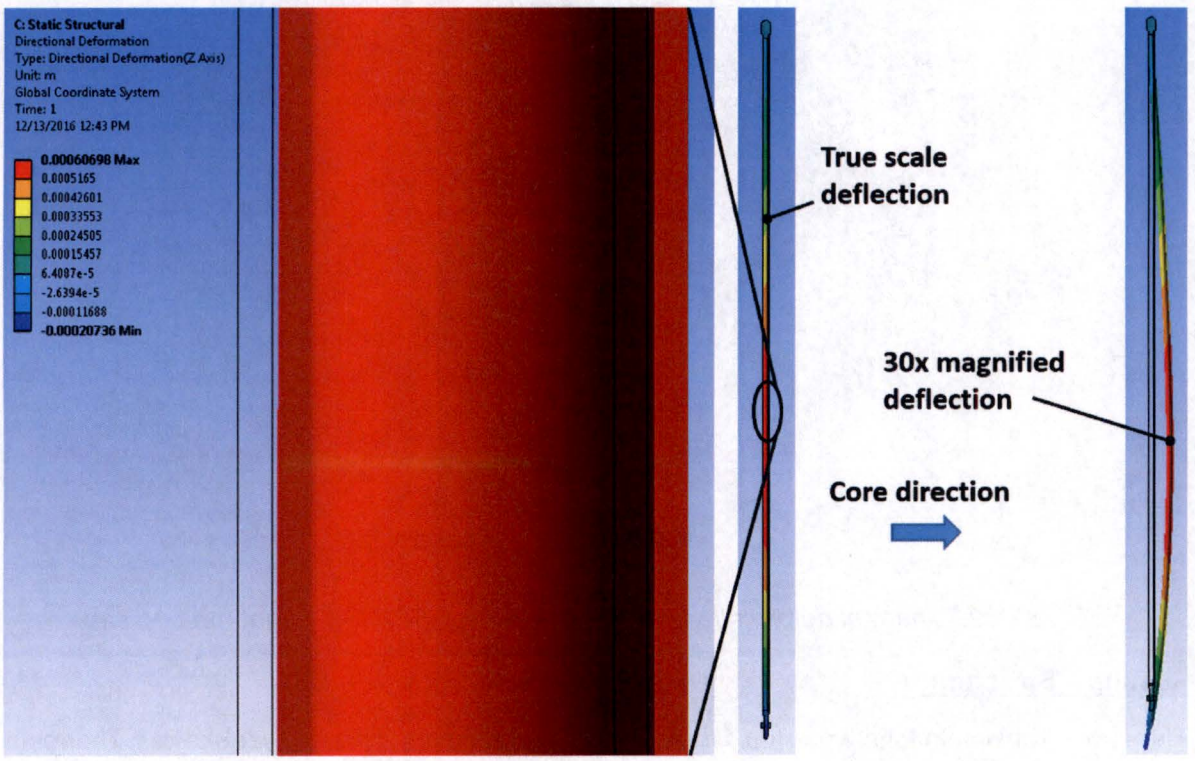

Figure 40. Deflection due to rod bowing for worst-case front-to-back power skew

Conclusion

The results of the combined thermal-structural analysis show that bowing of the rod due to directional skew of the power distribution within the UO_2 pellets is not a concern. Analysis predicts that in a worst-case scenario, the maximum horizontal deflection would be about 0.607 mm. Given the distance between the rod and the cartridge wall when centered is about 4.4 mm, no contact would be expected. Additionally, flow through the cartridge is highly turbulent and boundary layers are very thin, so this level of deflection would not affect the heat transfer [30441R00038, 30441R00033]. It must also be stated that the worst-case scenario is extremely conservative. The more realistic average power skew scenario predicts a deflection of only 60 microns, which would be virtually undetectable. Given these results, it can be concluded that rod bowing due to both thermal and irradiation effects will not affect the performance of the RB-MSS target rods or the system as a whole.

References

1. IAEA-TECDOC-1496, Thermophysical properties database of materials for light water reactors and heavy water reactors, International Atomic Energy Agency, June 2006.
2. ASME. II, Part B Non-Ferrous Material Specifications, Materials, New York: ASME 2015.
3. Rohsenow, W.M., Hartnett, J.P., Cho, Y.I., Handbook of Heat Transfer, 3rd Edition.

GENERAL ATOMICS
P.O. BOX 85608 SAN DIEGO, CA 92186-5608 (858) 455-3000